REVIEW

Check for updates

Nanomaterials in electrochemical nanobiosensors of miRNAs

Marziyeh Mousazadeh,[a] Maryam Daneshpour, [b,c] Saeed Rafizadeh Tafti, [d] Nahid Shoaie,[e] Fatemeh Jahanpeyma,[e] Faezeh Mousazadeh,[a] Fatemeh Khosravi,[d] Patricia Khashayar,*[f] Mostafa Azimzadeh [*d,g,h] and Ebrahim Mostafavi [*i]

Nanomaterial-based biosensors have received significant attention owing to their unique properties, especially enhanced sensitivity. Recent advancements in biomedical diagnosis have highlighted the role of microRNAs (miRNAs) as sensitive prognostic and diagnostic biomarkers for various diseases. Current diagnostics methods, however, need further improvements with regards to their sensitivity, mainly due to the low concentration levels of miRNAs in the body. The low limit of detection of nanomaterial-based biosensors has turned them into powerful tools for detecting and quantifying these biomarkers. Herein, we assemble an overview of recent developments in the application of different nanomaterials and nanostructures as miRNA electrochemical biosensing platforms, along with their pros and cons. The techniques are categorized based on the nanomaterial used.

[a]*Department of Nanobiotechnology, Faculty of Biological Sciences, Tarbiat Modares University, Tehran, Iran*

[b]*Biotechnology Department, School of Advanced Technologies in Medicine, Shahid Beheshti University of Medical Sciences, Tehran, Iran*

[c]*Livogen Pharmed, Research and Innovation Center, Tehran, Iran*

[d]*Medical Nanotechnology & Tissue Engineering Research Center, Yazd Reproductive Sciences Institute, Shahid Sadoughi University of Medical Sciences, 89195-999 Yazd, Iran. E-mail: m.azimzadeh@ssu.ac.ir*

[e]*Department of Biotechnology, Tarbiat Modares University of Medical Science, Tehran, Iran*

[f]*Center for Microsystems Technology, Imec and Ghent University, 9050 Ghent, Belgium. E-mail: patricia.khashayar@ugent.be*

[g]*Stem Cell Biology Research Center, Yazd Reproductive Sciences Institute, Shahid Sadoughi University of Medical Sciences, Yazd 89195-999 Yazd, Iran*

[h]*Department of Medical Biotechnology, School of Medicine, Shahid Sadoughi University of Medical Sciences, Yazd 89165-887, Iran*

[i]*Department of Medicine, Stanford University School of Medicine, Stanford, CA, 94305, USA. E-mail: ebimsv@stanford.edu, ebi.mostafavi@gmail.com*

1. Introduction

Biosensors and nanobiosensors have been widely used in medical diagnosis to quantify microRNAs (miRNAs) over the past decade.[1,2] miRNAs have become a valuable and reliable biomarker in diagnostic and therapeutic applications. miRNAs are known as small non-coding regulatory ribonucleic acids (RNAs) that have essential gene regulatory roles in main cellular functions, ranging from embryonic development, proliferation, apoptosis, and hematopoiesis to being linked to certain diseases, genetic disorders, and even cancer.[3] This is mainly because they are estimated to target more than 30% of the human genome responsible for important roles in cellular processes.[4]

Despite the shift toward their use as sensitive prognostic and diagnostic biomarkers for various diseases, miRNA detection has been challenging.[2] Because of their short length, miRNAs are difficult to amplify and are sometimes lost in conventional RNA isolation procedures. At the same time, they are highly homologous in sequence, making their detection challenging in terms of selectivity. In this regard, there is a need for better and more sensitive detection methods of miRNA. Deep sequencing, real-time polymerase chain reaction (RT-PCR), microarray, biosensors, and nanobiosensors are some of the commonly used techniques for quantifying miRNAs, and each of them has its pros and cons.[5]

Biosensors are categorized based on their transducers: electrochemical, optical, electrical, thermal, and mass-change sensors.[6,7] In the case of miRNA quantification, electrochemical methods are highly recommended owing to their high accuracy and considerable sensitivity.[8] Applying different nanomaterials in such biosensors can help improve certain features, particularly their sensitivity, by increasing the actual surface area, accelerating electron transfer rate, and producing a higher redox signal (to be used as the electrochemical label).[9,10]

Besides nanoparticles, nanopores[11] and nanochannels[12,13] have also been used in several electrochemical sensors for miRNA detection. The nanopore- and nanochannel-based biosensing platforms offer a high-throughput, ultrasensitive single-molecule sensing device capable of label-free detection and quantification of ultralow concentrations of the target.

Nanochannels perform better than nanopores with respect to selectivity, whereas the nanopore-based biosensors are easier to design and fabricate.[14]

As a result, focus has been shifted toward developing integrated nanopore/nanochannel devices as a result of the recent advancements in biology, microfluidics, microelectronics, and optical technologies.[14,15] However, specific challenges have limited their fabrication. The most important is keeping the target molecule inside the nanopore for an optimum interval known as the "goldilocks time" to reach the ideal detection accuracy. This is because most tiny molecules, such as miRNAs, leave the nanopores in a very short time, specifying the need for additional forces to store the molecule longer. These extra forces, however, may alter the nanopore structure, preventing the molecules from normal movement through the pores.[16–18]

Moreover, despite the promising results, the sensitivity of such sensing devices strongly depends on the temperature and pH because of the highly fragile nature of the nanopores/nanochannels. The variable non-uniform pore size can also restrict their practical application in different biomolecular fields.[18,19]

2. Nanomaterials and miRNA electrochemical sensors

In this section, we have categorized the electrochemical sensors for miRNA quantification based on the used nanomaterial and explained their specifications as well as pros and cons. Scheme 1 briefly represents the main nanomaterials

Scheme 1 Representation of main nanomaterials used in recent electrochemical nanobiosensors for miRNA quantification.

used to develop miRNA electrochemical biosensors according to our recent literature review, and they will be discussed in detail later in this article.

Fig. 1A and B, on the other hand, show the distribution of the miRNAs measured using nanobiosensors and electrochemical methods applied in these platforms, respectively. As seen, miR-21 is the most common target in such biosensing devices. This could be mainly because it was one of the first miRNAs detected in the human genome. It is upregulated in most known malignancies, including hepatocellular carcinoma, lung cancer, gastric cancer, lymphoma, glioma, and breast cancer.[20–23] Far behind it, miR-155, known as the master regulator of inflammation, can be seen in ref. 24. The limited number of studies on other miRNAs does not lessen the value of these markers. It should also be considered that redesigning the probes could make most miRNA biosensors compatible with other miRNAs.

Fig. 1B indicates the popularity of differential pulse voltammetry (DPV) among other electrochemical techniques for this application, mainly because of the higher sensitivity provided by this pulse technique. DPV and square wave voltammetry (SWV) are commonly used pulse techniques to quantify electroactive species. On the other hand, electrochemical impedance spectroscopy[25] is often used to characterize electrochemical systems. Cyclic voltammetry (CV) is the following linear method, mainly used for exploratory purposes.[26,27]

2.1. Carbon-based nanomaterials in miRNA biosensor

Although the first carbon-based molecules, namely, fullerenes, were discovered in 1985, graphene-based nanomaterials are currently the leading material in various applications, such as

Ebrahim Mostafavi

Dr Ebrahim Mostafavi has so far received training at Stanford University School of Medicine (PostDoc), Northeastern University (Ph.D.), Harvard Medical School (Researcher), and University of Tehran (M.Sc. and B.Sc.). His research interests revolve around the engineering and development of (nano)biomaterials, nanocarriers, and 3D in vitro models (hydrogels, 3D bioprinted constructs, nanofibrous scaffolds, organoids, vascular grafts, and microfluidic systems) to create biologically complex systems for a range of applications such as tissue engineering and regenerative medicine, translational medicine, cancer therapy (with focus on women's cancer), biosensing, and infectious diseases. Dr Mostafavi serves as Associate Editor-in-Chief of several prestigious and high-impact journals of Elsevier, Springer, Cell Press, Dove Medical Press, T&F, Frontiers, etc. He is also an Editorial Board Member of 30+ impactful and prestigious biomedical and materials science journals.
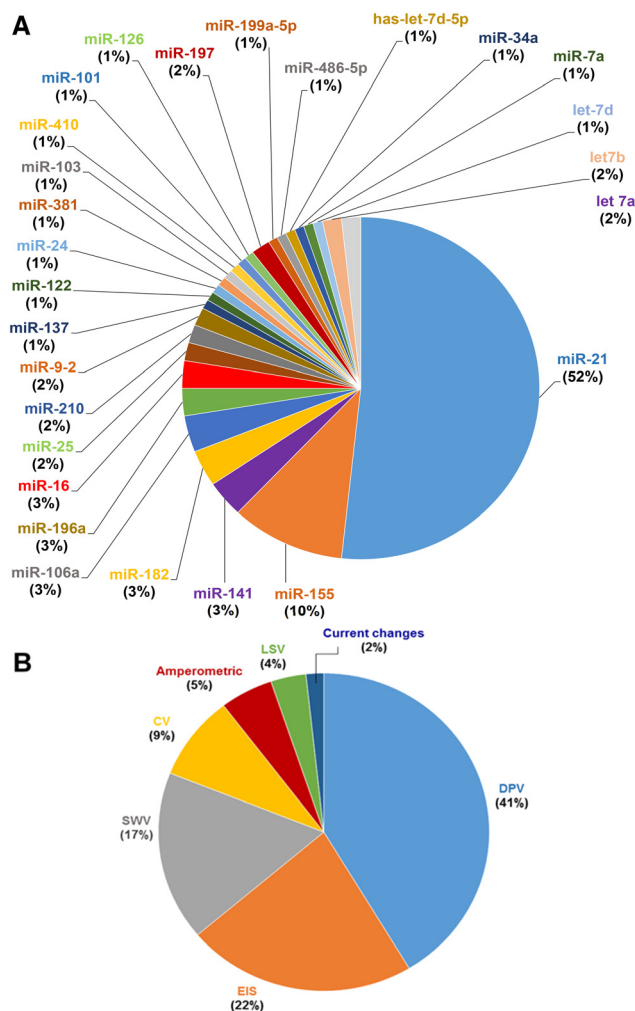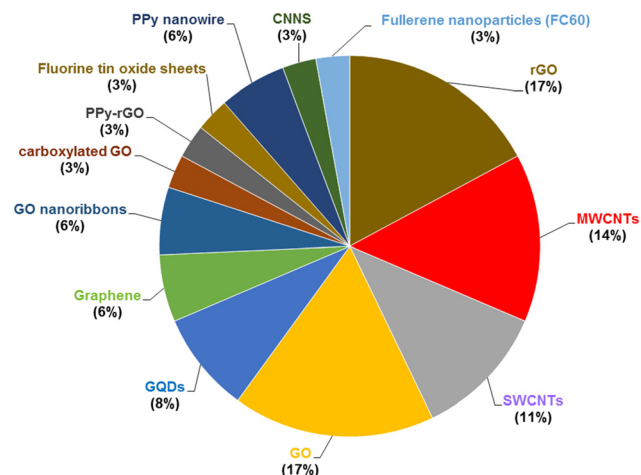
Fig. 1 Pie chart showing the distribution of common miRNAs (A) and electrochemical methods (B) reported in recent articles based on miRNA biosensors.

Fig. 2 Pie chart showing the distribution of carbon nanomaterials applied in recent articles based on miRNA biosensors.

sensors.[28] Since its discovery in 2004, graphene has gained tremendous attraction, and later, graphene oxide (GO) and other reduced GO (rGO) became the main carbon nanomaterials used in electrochemical nanobiosensor fabrication (Fig. 2). It is worth highlighting that graphene-based nanomaterials have been used in more than 60% of the reported miRNA biosensors.

2.1.1. Graphene family. Graphene and graphene-based nanomaterials have specific physical, chemical, and electrical properties. They are popular in the biosensor field because they provide a biocompatible high surface area. They acceptably adapt to different functionalizing approaches with biomolecules like DNA, enzymes, and antibodies.[29]

As one of the most popular graphene family members, GO has specific compatibility, water solubility, electrochemical, and catalytic properties. These criteria make graphene suitable for electrochemical sensors.[30] Carbon nanostructures and nanoparticles have thus been used to improve miRNA sensing by enhancing the sensor's active surface area, the quality of

miRNA attachment to the electrode, total conductivity, sensitivity, and selectivity.[31,32] In most of these studies, microRNA-21 was used as a target linked with several diseases, such as cancer, especially breast malignancies. Two main fabrication methods were reported in this regard. The most prevalent one was the deposition of the nanostructures and nanoparticles on the electrode surface, aiming to improve miRNA attachment as well as the electrode's electrical conductivity. In the other technique, the nanoparticles were added to the miRNAs rather than used in electrode surface modification. Table 1 outlines the papers reporting surface treatment methods using carbon nanostructures or other nanoparticle combinations.

During the surface modification step, the role of graphene is critical for preparing a nano-editable flat-shaped surface with excellent electrical properties.[33,34] Using graphene in combination with other nanomaterials helps with three main goals: enhancing electrode electrical conductivity (by adding gold or silver nanoparticles[35]), increasing the sensor active surface area, and improving miRNA attachment to the surface using a designed H-bond chain.[36] In this regard, the use of gold nanoparticles (AuNPs) in conjugation with tungsten oxide–graphene composites is reported to result in low limit of detection values (limit of detection (LOD) = 0.05 fM).[37] A perfect-match signal amplification method also helped with low LOD and high sensitivity. In this system, the redox chain reaction was catalyzed by the streptavidin conjugated to alkaline phosphates attached to the strands on the electrode. It was later easily detached in the presence of the complementary miRNA.

The process involved attaching two hairpin DNA strands to the electrode's WO$_3$–graphene and Au nanoparticle composites. One strand was first attached to the surface and hybridized in the presence of the miRNA. The addition of the second strand resulted in the detachment of the miRNAs from the first strand due to the formation of longer pins and stron-

Table 1 Electrochemical miRNA biosensors that use graphene and its family

miRNAs	Nano structures	Mechanisms and advantages	Concentration range	Detection limit	Ref.
miR-21	Fluorine tin oxide sheets, carboxylated GO, gold, PtNPs	NH_2 streptavidin-carboxylated complementary strands	1 fM–1 μM	1 fM	36
miR-16	PPy–rGO and AuNPs	Electropolymerization to combine PPy and rGO	10 fM–5 nM	1.57 fM	31
miR-21	MWCNTs, GO nanoribbons, AuNPs	Nuclease-based target recycling and alkaline phosphatase	0.1 fM–0.1 nM	0.034 fM	42
miR-137	SPCE, GNW, rGO	A combination of GNW and GO	5 fM–750 fM	1.7 fM	38
miR-21	ZrO_2-reduced GO nanohybrids	Catalytic hairpin assembly	10 fM–0.1 nM	4.3 fM	43
miR-221	rGO flakes and AuNPs on SPCE	Porous structure of electrodes due to RGO flakes	4 pM–10 nM	0.7 pM	34
miR-21	GO-loaded iron oxide	Supermagnetic nanoparticles by adding iron oxide	1 fM–1 nM	1.0 fM	44
miR-21	AgNPs polyaniline, graphene	Polyaniline	10 fM–10 μM	0.2 fM	35
miR-21	Tungsten oxide, graphene, and AuNPs	Hairpin-based target recycling, enzymatic signal amplification	0.1 fM–100 pM	0.05 fM	37
miR-21	rGO and AuNPs	miRNA hinders charge transfer in the modified electrode	18 fM–2 pM	5.4 fM	39
miR-21	rGO and AuNP	Capture DNA–AuNPs conjugated Fc	10 fM–2 pM	5 fM	40
miR-210, miR-155, miR-21	AuNPs/GQDs/GO	DNA probes–AuNPs/GQDs/GO-modified SPCE	0.001 pM–1000 pM	0.04, 0.33, 0.28 fM	41

AuNP: gold nanoparticles, SPCE: screen-printed carbon electrodes, GO: graphene oxide, GQD: graphene quantum dots, rGO: reduced graphene oxide, PtNPs: platinum nanoparticles, MWCNTs: multiwalled carbon nanotubes, GNR: gold nanorods, AgNPs: silver nanoparticles, GNR: gold nanorod, GNW: gold nanowire.

ger bonds. This is the recycling of miRNA from the solution to another strand. Hence, the promising results in this system were obtained through the combination of target recycling, signal amplification, and surface modification with nanomaterials.

As another example, Bharti et al. added carboxyl groups with fluorine tin oxide and Au–Pt nanoparticles to a GO sheet.[36] In this system, the streptavidin NH_2 groups conjugated to the surface receptor provided a biotinylated capture probe complementary to the target, resulting in a significant change in the current specific to miRNA 21 (Fig. 3A).

Compared to miRNA treatments, amplifications, and medium alterations using nanomaterials, the main advantage of the electrode surface treatment methods is their relatively lower costs. Moreover, using screen-printed carbon electrodes (SPCE) and treating the conductive carbon layer using different nanomaterials helped reduce costs. For instance, Azimzadeh et al. used electrochemically-reduced GO with gold nanowires to increase the interaction surface area as well as that significantly. Using these low-cost modifications, the LOD of the sensor reached 1.7 fM.[38]

In an alternative attempt, rGO was functionalized with pyrene carboxylic acid (PCA) bonded to the DNA capture probe through its amino terminals. AuNPs were coated with 6-ferrocenylhexanethiol (Fc-SH) as the signaling molecules, generating an oxidation peak in the electrochemical response. The existence of miRNA-21 promoted the formation of the DNA/RNA complex of the capture probes with the target miRNA while reducing the charge transfer rate and the DPV signals. On the other hand, higher responses were achieved in the absence of the target miRNA-21. The incubation time for the sensor was 30 minutes, and the results showed an LOD of 5.4

fM while the linear range was 18 fM–2.0 pM for this nanobiosensor. In addition, it could successfully detect miRNA with good selectivity in both breast cancer cells and serum without the need for additional extraction or amplification steps.[39]

Zouari et al. advanced a sandwich assay between the captured SH-DNA attached to the electrode surface, miRNA-21, and biotinylated DNA. The electrode surface was already modified with rGO and AuNPs before adding the streptavidin–ferrocene (Fc)–AuNPs. The bond between these NPs and the biotinylated DNA resulted in high DPV signals. The platform had a linear range between 10 fM–2 pM and an LOD of 5 fM. This highly sensitive and selective sensor was also reported to remain stable for two months, which is important for future applications (Fig. 3B).[40]

Elsewhere, the methods for response enhancement aimed to improve the conductivity of the electrode, recycling, and the quality of electron transfer between the nanostructures and the electrode surface were used for classification purposes. Salahandish et al. applied a sandwich of AgNPs between polyaniline and nitrogen-doped functionalized graphene in this regard. This three-layer composite combined with several carboxyl groups already immobilized on a rough polyaniline surface provided a perfect charge transfer response and significantly increased the sensor's sensitivity. The possibility of being combined with recycling or enzymatic and other biochemical strategies was another advantage of this sensor.[35]

In another study, three miRNAs were detected simultaneously. AuNPs, GQDs (graphene quantum dots), and GO were cast on the SPCE, which were modified by polydopamine (PDA), anthraquinone (AQ), and methylene blue (MB). Using SWV, the sensor had a dynamic range of 0.001–1000 pM, and the LODs were 0.04 fM (miR-21), 0.33 fM (miR-155), and 0.28
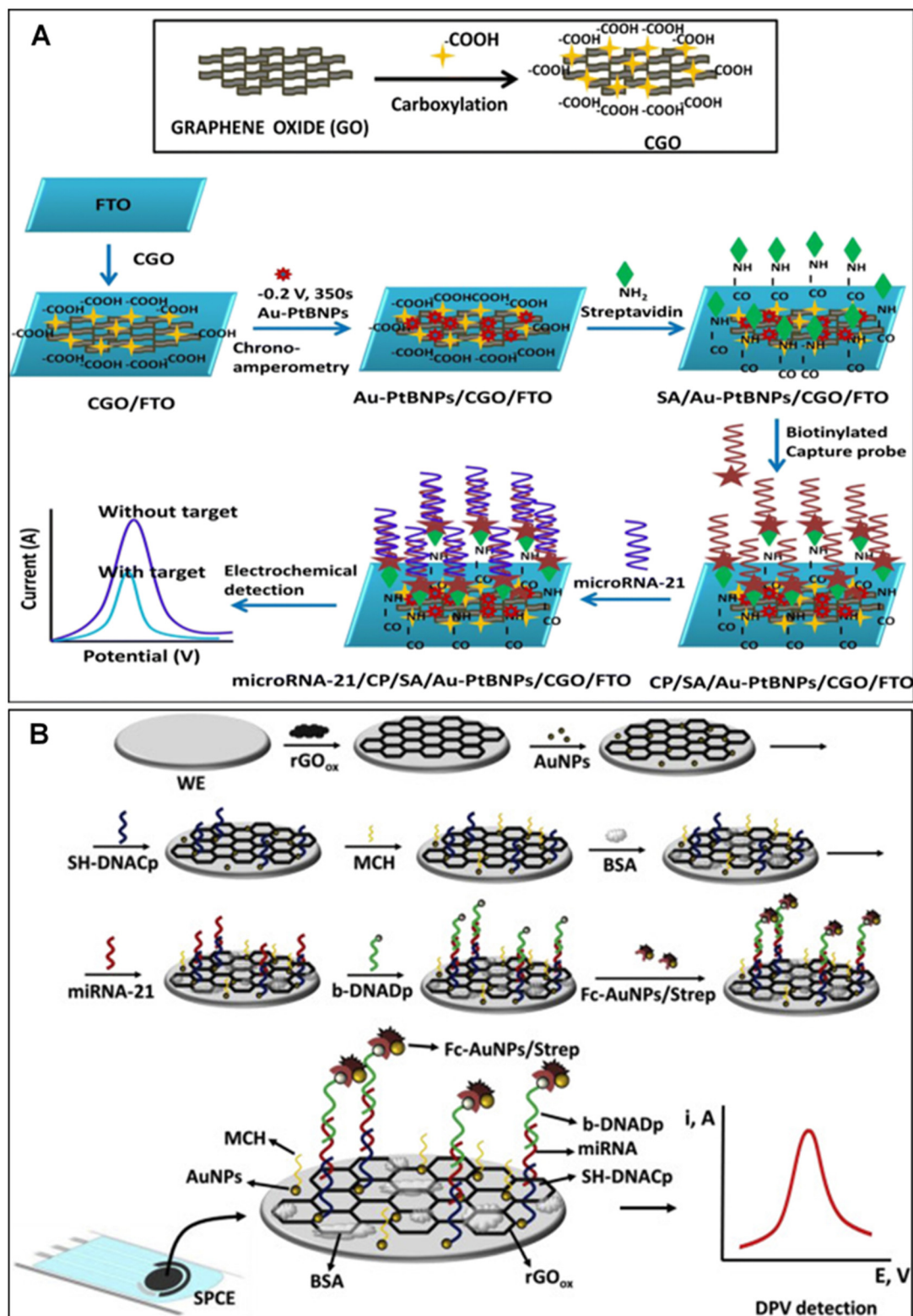
Fig. 3 Electrochemical sensors for miR-21 detection (A) developed by combining the carboxyl groups, NH$_2$ streptavidin, and Au-nanoparticles[36] (B) based on the rGO and AuNPs.[40]

fM (miR-210). Being multiplex, accurate, and compatible with real samples were the other noteworthy features of this platform.[41]

Graphene and its derivatives have a long list of properties, including an ideal surface physiochemistry and electronic structure, a large surface area providing access to active sites

and resulting in high loading capacities, and a mediator-free transfer of electrons between the functionalized graphene and the bioreceptor. These features have made them attractive for rapid, sensitive, selective, economic analytical biosensing devices for miRNA analysis.[45–47]

This is because most of the reported miRNA biosensors, fabricated using graphene nanomaterials, have complex fabrication and detection steps, with many requiring sample pre-treatment and extraction processes. Moreover, to achieve the required limit of detection for miRNA detection, the graphene nanomaterials need to be combined with Au- or Ag-nano-structures that considerably increase the cost.

In contrast, batch-to-batch variation in the graphene quality (also graphene derivatives) is another challenge concerning nanobiosensor sensitivity. This is mainly because even minimal structural alterations can lead to different specifications of graphene nanomaterials. The orientation of graphene nanomaterial sheets exposed to biomolecules, number of synthesized layers, active sites, and oxidation state of these materials are among other features with a direct impact on the critical performance parameters of the nanobiosensors, suggesting the robustness of the graphene nanomaterials' synthesis process as the most crucial step in the fabrication of such miRNA biosensors.[29,48]

It can be inferred that the success of miRNA detection using sensors hinges on a variety of factors, including the combination of nanomaterials and nanoparticles, recycling strategies for developing new nanocomposites, enhancing H-bond specificities with biochemical reagents, and performing miRNA treatment and amplification. Among the materials available, the graphene family stands out due to its exceptional conductivity, large surface area, and ease of functionalization, making it a preferred choice for achieving enhanced sensitivity and selectivity in miRNA biosensors. However, costs associated with production may be relatively high, and challenges related to the aggregation and dispersion of graphene sheets must be handled carefully.

2.1.2. Nanotubes and nanofibers. Electrode surface treatment using carbon nanotubes can enhance the LOD.[49] CNTs are carbon-based materials consisting of graphene sheets with diameters less than 50 nm. They have electronic, thermal, and mechanical properties because of their highly oriented structure. Carbon nanofibers are composed of graphene sheets as stacked layers with diameters of the order of nm and lengths of the order of μm. These one-dimensional carbon nano-structures have great applications in diagnostics.[50] Due to the flexible nature of CNTs, besides their conductivity and mechanical strength, these nanoparticles are used in different electrochemical sensors, such as fabricating stretchable electrodes for electrochemical sensor applications.[51]

The advantages of graphene and CNTs over each other would boil down to a surficial shape, controlled fabrication process, cleaner carbon fabrication context, being one-dimensional for graphene and two-dimensional conductivity, and a strand-like shape for CNT. While graphene is better for surface treatment and CNT is more applicable for the attachment to the DNA strands using different conjugation methods, both have approximately the same effects on the electron transfer rate. This is because the CNTs are more appropriate for miRNA attachment and provide more enhanced choices due to their pin-like structure. These nanomaterials can also be used in combination with other nanoparticles and molecules. The recent studies on carbon nanotubes and nanofibers are summarized in Table 2.

Using carbon nanotubes as pins for miRNA attachment through the carboxyl and amino groups has shown promising results. Hu et al. described adding amino and carboxyl groups to the tips of the CNTs, resulting in perfect attachment to the complementary strands.[52] Using a sequence-specific hairpin strand displacement strategy for signal amplification, they reached an LOD of 56.7 aM.

Some studies have used shortened CNTs because of their top open-hallow structures, favorable for DNA fragments, and fast electron shuttle to increase conductivity.[49] In this regard, Deng et al. incorporated thionin on the shortened and acidified CNTs loaded with miRNA on one side and AuNPs on the other, then covered the electrode with 6-mercaptohexanol (MCH) to fill the gaps between probes and the complementary strand. The attachment of the complementary strands created a highly conductive path for the transfer of electrons from the medium to the working electrode through the CNTs and AuNPs. This was the reason behind the sharp current response recorded in the presence of the specific miRNA (LOD = 0.032 pM). While expensive reagents were not necessary, the need for a preparation step for functionalizing the CNTs with thionin and the strands complicated the method. Moreover,

Table 2 Electrochemical sensors based on nanotubes and nanofibers for miRNA detection

miRNAs	Nano structures	Mechanisms and advantages	Concentration range	Detection limit	Ref.
miR-21	MWCNTs–GO nanoribbons–AuNPs	Target recycling using enzyme and alkaline phosphatase	0.1 fM–0.1 nM	0.034 fM	42
miR-21	SWCNTs	T7 exonuclease assisted target recycling	0.01–100 pM	3.5 fM	56
miR-21	Shortened and acidified MWCNTs with AuNPs	Multiwalled carbon nanotubes (S-MWCNTs)	0.1–12 000 pM	0.03 pM	49
miR-21	Carboxylated MWCNTs	Non-enzymatic amplification using hairpin strand displacement	0.1 fM–5 pM	56.7 aM	52
miR-21	CNTs, AuNPs	miRNA opened bio-gates to the nanopores	0.1–1000 fM	2.7 aM	53
miR-24	MWCNTs–PPy nanowires	PPy/MWCNTs/PB NPs–miRNA hybridization	0.1 pM–1 nM	33.4 fM	55

similar works have been reported using such target recycling strategies to enhance the sensor.

Wang *et al.* applied a combination of GO nano-ribbons, multiwalled CNTs, and AuNPs along with duplex-specific nuclease to form the recycled strands. This technique for miRNA detection achieved an LOD of 0.034 fM.[42] Another strategy for reaching low LOD in sensors is using negatively controlled biochemical mechanisms, such as streptavidin with conjugated alkaline phosphates (SA-ALP) enclosed in the immobilized probe. In case the miRNA-21 is not present, the SA-ALP catalyzes the process of ascorbic acid (AA) production from ascorbic acid-2-phosphate (AAP), which triggers the iodine redox reaction and creates a significant response of electrochemical output. In case DNA is available, the complementary strand was hybridized, removing the duplex using duplex-specific nuclease, and causing the detachment of the SA-ALPs. This resulted in a reduction in the electrochemical signal. Despite the drawback of using various chemicals and enzymes, a great LOD was achieved.

Gai *et al.*, through a creative nano-gating mechanism, detected specific miRNAs.[53] If the target miRNAs are available, the nano-cells filled with the acceptor ion open due to the nano-biogates containing a complementary DNA to the target. Therefore, stronger H-bonds are formed between the complementary strands, overcoming previous cage-gating molecular bonds and helping the complementary miRNA molecules release a fixed number of acceptor ions in the medium, which could later be detected using regular sensing electrodes. In such a manner, an LOD 3 times lower than that of standard surface treatment methods was achieved (LOD = 2.7 aM). Hence, this was considered a significant move forward in using carbon-based nanomaterials for miRNA detection.

Despite growing interest in surface functionalization methods, several studies have focused on factors other than only electrode-miRNA conjugation and conductivity.[54]

In a study by Yang *et al.*, a dual signal amplification biosensor was developed based on a nanowire array using multiwalled carbon nanotubes with the polypyrrole (PPy) (PPY/ MWCNTs) and GCE. The attachment of DNA and miRNA altered the conductivity and oxidation peaks due to the presence of CNTs and Prussian blue, respectively. The sensor showed an LOD of 33.4 fM and a linear response between 0.1 pM and 1 nM. The sensor was simple, easy to operate, and sensitive.[55]

CNTs-based biosensors are promising based on their outstanding mechanical properties, high surface area, ideal electrical conductivity, stable activity in aqueous and nonaqueous solutions, and great thermal conductivity. There are, however, several practical challenges, including the size control of CNTs while manufacturing. In the case of realistic commercial applications, producing CNTs with high purity and reasonable prices has been the main issue in recent years. In CNT-based biosensors, the immobilization process of biological materials may damage the biological activity, biocompatibility, and structure of CNTs. In addition, due to their nature, CNTs are likely to interact with other macromolecules, especially surface

proteins. Hence, analyzing the real samples using CNT-based biosensors may be biased due to the background noise and false positive results.[57] In summary, CNTs and CNFs exhibit high aspect ratios, quick electron transfer, and mechanical durability, contributing to improved sensitivity. However, there are still challenges, such as the possibility of agglomeration, and it may be necessary to have precise control over their properties to ensure consistent performance.

2.1.3. Other carbon-based NPs. Although carbon nanotubes, graphene, and GO are the most famous nanomaterials made from carbon commonly applied as working electrodes in electrochemical sensors,[58] other members like carbon dots, fullerenes, and composites of graphene and other nanoparticles have also been used in sensing platforms. Nanodiamonds are carbon-based nanostructures used in electrochemical sensors because they have a higher surface area and electrocatalytic activity.[59] Another example is carbon nitride nanosheets (CNNS) combined with AuNPs and cast on the GCE. In this sensor, the captured thiolated DNA bonded to the electrode surface *via* Au–SH bonds. Methylene blue (MB) was coupled to another end of the captured DNA, generating high and robust electrochemical SWV signals. In case miRNA-21 is present, DNA/miRNA is attached to each other, and subsequently, duplex-specific nucleases (DSN) are utilized to digest the DNA and release MB molecules. After washing the electrode, a lower SWV response was noted because of the reduced number of MB molecules (Fig. 4A). This sensor shows high sensitivity and reproducibility in real samples (serum). The dynamic range was from 10 fM to 1 nM, while the LOD was 2.9 fM.[60]

While graphene mainly covers the whole electrode surface and develops a highly conductive sheet, Hu *et al.* added graphene quantum dots to a gold sheet instead of amplifying the enzyme catalysis.[61] This is another successful example of enhancing the catalytic reactions and activating the surface. The sensor had an LOD of 0.14 fM.

Graphene dots are cheap, easily accessible, biocompatible small and zero-dimensional carbon-based nanoparticles with high surface-to-area ratios. Farshchi *et al.* introduced a paper-based electrochemical sensor for miRNA-21.[62] Paper-based analytical devices have gained considerable attention in bioanalytical point-of-care (POC) platforms due to advantages such as lightweight, being inexpensive, flexible, biocompatible, biodegradable, easy to operate and construct, and environment friendly.[63,64] Their platform used silver–gold core–shell nanoparticles conjugated with quantum dots of graphene (core–shell Ag@Au/GQDs) as a nano-ink for electrode printing. A peptide nucleic acid[65] sequence with a high affinity for miRNA-21 was attached to the electrode. The reported linearity and LOQ of the sensor were 5 pM to 5 μM and 5 pM, respectively. The reported sensor was simple, and the high flexibility of the paper made it suitable for small and wearable sensors.

Dual signal amplification strategies have attracted attention in fabricating sensitive electrochemical biosensors. Adapting this approach, a biosensor was presented for miR-141 detection as a potential prostate cancer biomarker. In this regard, the Au electrode was first coated with NH_2–SH-functionalized

Fig. 4 Electrochemical sensor (A) based on the AuNP- and CNNS-modified electrode for miRNA-21 detection.[60] (B) Electrochemical sensor based on the n-doped laser-induced graphene for miR-486-5p detection.[67]

fullerene nanoparticles (FC60), which improved binding through Au–SH bonds. On the other side, two different DNAs (azide-strand and alkaline strand) were mixed and catalyzed to custom a G-quadruplex DNA complex and drop cast over the modified electrode. The alkaline-strand hairpin structure opened with the target miRNA, permitting them to bond. After that, duplex-specific nucleases (DSN) were used to digest DNA in the complex of DNA/RNA. During this procedure, miRNA-141 was released to generate higher signals. The addition of hemin to the system helped achieve HRP-like results. The sensor had a dynamic range between 0.1 pM and 100 nM, while the LOD was 7.78 fM.[66]

miR-486-5p was another example detected *via* a sensor developed by Wan *et al.* A CO_2 laser was used to print the laser-induced graphene (LIG) electrode on a polyimide (PI) paper. The nitrogen-doped LIG sensor was highly sensitive for nucleic acid detection. The hybridization of target miRNA and CPs reduced the current generated by the $[Fe(CN)_6]^{3-/4-}$ redox complex (Fig. 4B). The linearity and LOD of the as-described LIG sensor were 10 fM toward 10 nM and 10 fM. The desired power of up to 80 W for LIG fabrication was achieved in a single step. This low-cost platform was sensitive and easy to fabricate.[67] The information on research about GQDs and other carbon nanostructures is summarized in Table 3.

Table 3 Electrochemical miRNA biosensors based on carbon nanomaterials

miRNAs	Nano structures	Mechanisms and advantages	Concentration range	Detection limit	Ref.
miR-155, miR-210, miR-21	AuNPs/GQDs/GO	AuNPs/GQDs/GO-modified SPCE	0.001 pM–1000 pM	0.04, 0.33, 0.28 fM	41
miR-21	AuNPs and CNNS	Capture DNA–MB	10 fM–1 nM	2.9 fM	60
miR-155	Gold electrode–GQDs	Enzyme catalytic amplification	1 fM–100 pM	0.14 fM	61
miR-21	Core–shell of Ag@Au/GQD	PNA on the paper-based electrode	5 pM–5 μM	5 pM	62
miR-141	Fullerene nanoparticles (FC60)	EATR-G-quadruplex DNA on FC60–Au electrode	0.1 pM–100 nM	7.78 fM	66
miR-486	N-doped laser-induced graphene	miRNA attachment to the LIG surface	10 fM–10 nM	10 fM	67

SPCE: screen-printed carbon electrode (SPCE), Fc: ferrocene, rGO: reduced graphene oxide, AuNPs: gold nanoparticles, DPV: differential pulse voltammetry, EATR: enzyme-assisted target recycling, EIS: electrochemical impedance spectroscopy, GQD: graphene quantum dots, SWA: square wave voltammetry, PNA: peptide nucleic acid, CNNS: carbon nitride nanosheet, LIG: laser-induced graphene. MB: methylene blue.

The biosensor-friendly properties of graphene quantum dots (GQDs) have made them an attractive candidate for use in biosensors. However, developing a scalable and simple synthesis method for high-quality GQDs remains a significant challenge. The procedure involves several critical steps, such as size control, crystallinity, doping, and surface functionalization regulation, which are known to influence the final specifications of the GQDs and, consequently, the biosensor's performance. The successful synthesis of high-quality GQDs could significantly enhance the biosensor sensitivity and accuracy.[68]

2.2. Metal nanomaterials in miRNA biosensors

Metals are considered the most diverse group of nanomaterials used in biosensor applications. The free active electrons of this class of materials and their notable characteristics at the nanoscale have made them ideal candidates in this regard. Gold nanostructures with unique capabilities and extraordinary biocompatibility, followed by silver nanoparticles and magnetic iron oxide nanostructures, offer higher efficiency, particularly in electrochemical sensing systems (Fig. 5).

2.2.1. AuNPs and composites. AuNPs have gained increasing interest in various chemical and biomedical applications, especially biosensing. Various studies have discussed a significant improvement in performance and signal amplification when using these nanostructures (Table 4).[69] AuNPs are commonly used in optical and electrochemical sensors due to their high surface-to-area ratio, simple functionalization, high catalytical activity, and biocompatibility. These nanoparticles are frequently reported as suitable transducers for reducing the sensors' detection limit.[70] The application of AuNPs in electrochemical sensors increases the electrical conductivity. Furthermore, mixing AuNPs with other materials and nanoparticles makes them suitable and highly used particles in electrochemical sensors.[71] The unique properties of AuNPs, such as enhanced electrical, catalytic, and surface plasmon resonance (SPR) properties, fluorescent quenching activities, biocompatibility, low toxicity, and high stability, have made them promising candidates for, but not limited to, electrochemical, colorimetric, florescence-based, SPR-based, and lateral/vertical flow sensors.[69,72]

Using functionalized AuNPs alone or combined with other nanomaterials to enhance the sensitivity has become remarkably interesting over the past years. The combination of AuNPs with magnetic microbeads (MMBs) has demonstrated exceptional properties such as special magnetic properties, enhanced conductivity, and enlarged surface area.[73] Lu *et al.* introduced a voltammetric measurement system using a combination of AuNP-coated MMBs (AuNP-MMBs) and Fc-covered AuNPs/streptavidin to amplify and then detect miR-182. The AuNP-MMBs were configured to conjugate with high-density hairpin-structured DNA probes. With the target miRNA, biotinylated hairpin DNA probes will be open, followed by the hybridization of miRNAs with the loop region. A new assembly was formed from the attachment of (Fc)-capped AuNPs/streptavidin conjugates with the biotinylated DNA hairpin probes. The generated assemblies were magnetically adsorbed on the magnetic electrode for voltammetric measurements. Using this system, miR-182 concentrations as low as 0.14 fM were selectively and reproducibly detected without extraction or PCR procedures. Using AuNP-MMBs improved the conductivity, chance of target hybridization, and detection limit while facilitating the magnetic separation step.[73]

Wang *et al.* used AuNP-MMBs and diblock oligonucleotide (ODN)-functionalized AuNPs to develop a multiplex electrochemical miRNA detection system. The ODN-modified AuNPs were applied to improve the hybridization efficiency due to a recognition and a polyA anchoring tail. The AuNP-MMBs were configured to retain hairpin-structured probes and unfold in the case of availability of the target miRNAs. In this regard, the ODN-modified AuNPs are attached to the target miRNAs. miR-182 and miR-381 were thus detected simultaneously with MB and Fc tags of the ODNs. Using this system, the LODs were 0.20 fM and 0.12 fM for miR-182 and miR-381, respectively.[74]

In a recent study, a biosensor was developed for miR-21 detection using an AuNPs/hollow molybdenum disulfide (MoS_2) microcubes (AuNPs/MoS_2)-modified electrode.[20] This work used AuNPs as the sensing substrate to immobilize large amounts of DNA probes, which subsequently helped lower the LOD. The three strategies employed for signal amplification include enzyme signal amplification, duplex-specific nuclease

Fig. 5 Pie chart showing the distribution of metal nanomaterials in recent articles based on miRNA biosensors.

Table 4 The electrochemical biosensors based on AuNPs for miRNA detection

miRNA	Nanoparticles and electrode modifications	Electrochemical method	Linear range	Detection limit	Ref.
miR-182	Magnetic electrodes + AuNP MMBs	CVs	5–100 fM	0.14 fM	73
miR-182; miR-381	AuNP–MMBs + diblock oligonucleotide–AuNPs	DPV	5–600 fM; 1–800 fM	0.20 fM; 0.12 fM	74
miR-21	AuNPs + molybdenum disulfide microcubes	DPV	0.1–0.1 pM	0.086 fM	20
miR-21	Bridge DNA AuNPs	EIS	10^{-17} to 10^{-11} M	6.8 aM	78
let-7d	Doxorubicin loaded AuNPs + gold electrode	SWV	1 pM–10 nM	0.17 pM	81
miR-21	DNA–gold nanoflower + platinum electrode	DPV	1 μM–50 pM	135 aM	88
miR-103	AuNPs + JUG-SH/6-MHA SAM + GCE	SWV	100 fM–5 nM	100 fM	86
miR-155	AuNPs-paper electrode + AuNPs-modified Cu-MOFs	DPV	1.0 fM–10 nM	0.35 fM	63
miR-21	SWCNTs + PNA probe + dendritic nano gold	DPV	0.01 fM–1 μM	0.01 fM	90
miR-21	AuNPs and CNNS	SWV	10 fM–1 nM	2.9 fM	60
miR-21	Stacking probe + gold nanostructure + SPCE	Amperometry	10 fM–1 nM	7.5 fM	91
miR-410	AuNP/PNT nanocomposite + graphite electrode	EIS	10–300 pM	3.9 fM	92
miR-21	PPY/GP composite + MB + AuNPs + SPCE electrode	DPV	1.0–1.0 nM	0.020 fM	93
miR-101	Gold nanodendrites + Pt + Ag electrode	SWV	10^{-10} to 10^{-7} M	91.4 pM	94
miR-106a, let-7a	AuNPs, CdSe@CdS quantum dots, GO	DPV	0.1–5000 fM	0.06 fM 0.02 fM	96

CVs: cyclic voltammograms; DPV: differential pulse voltammetry; MMB: magnetic micro beads; SWV: square wave voltammetry; EIS: electrical impedance spectroscopy; SWV: square wave voltammetry; SPCE: screen printed carbon electrode; GCE: glassy carbon electrode; JUG-SH: 5-hydroxy-3-hexanedithiol-1,4-naphthoquinone; 6-MHA: 6-mercaptohexanoic acid; SAM: self-assembled monolayer; CuMOFs: modified Cu-based metal–organic frameworks; MoS$_2$: molybdenum disulfide; MCH: mercaptohexanol; SWCNTs: single-wall carbon nanotubes; FTO: fluorine-doped tin oxide; MU: mercapto undecanol; PNA: peptide nucleic acid; AuNPs: gold nanoparticles; PNT: peptide nanotubes; GP: graphene; PPY: polypyrrole; MB: methylene blue; CNNS: carbon nitride nanosheet; Pt: platinum; Ag: silver.

(DSN), and finally, electrochemical–chemical–chemical (EEC) redox cycling. The biotinylated capture probes hybridized with the analyte (miR-21), forming duplexes later cleaved by DSN. Upon cleavage, miR-21 was recycled, and the exposed biotin tags were attached to SA-ALP. When ascorbic acid is present, EEC redox cycling is induced, leading to the generation of electrochemical response. Therefore, the detection of miR-21 in human serum had the dynamic range of 0.1 fM–0.1 pM and 0.086 fM LOD.[20]

Similar to the conventional methods, the majority of miRNA detection approaches have low sensitivity.[75–77] Using bridge DNA–AuNPs and target-triggered cyclic duplex-specific nuclease digestion, Bo et al. reported a three-way signal amplification method for ultrasensitive miR-21 detection. Bridge DNA–AuNPs were constructed using two thiolated DNA probes and 2 DNA bridge probes linking three AuNPs. When miR-21 was present in the sample, the hairpins were opened, and an RNA/DNA duplex was formed. The duplex structure was subsequently recognized and digested by DSN, resulting in the release and recycling of miRNAs. The remaining DNA–AuNPs generate a measurable electrochemical response. The proposed biosensor exhibited a dose-dependent response in the dynamic range of 10^{-17} to 10^{-11} M and an LOD of 6.8 aM with no need for reverse transcription or pre-amplification steps.[78]

In another study, Tang et al. employed a simple dual-signal enhancement strategy for a nanobiosensor in miR-16 detection. The nanobiosensor, constructed on the surface of a single Au nanowire electrode (SAuNWE), was a "signal-on/-off" system during the hybridization/de-hybridization processes. The biosensor was assembled by immobilizing hairpin capture probes and harbor ring methylene blue tags (MB-CP) on the surface of SAuNWE. The MB-CPs were then hybridized with Fc-labeled aptamer probes (Fc-CPs) complementary to miR-16. In the presence of miR-16, the Fc-CPs were dissociated, leading to the recovery of the hairpin structures. Fc and MB contributed to generating electrochemical signals upon the hybridization/de-hybridization processes. This nanobiosensor detected target miR-16 levels with an LOD of 16 fM and linear range of 0.1 pM–100 nM in 2 h (including RNA extraction procedure).[79]

Li et al. used a cyclic enzymatic amplification method (CEAM) in the ultra-sensitive electrochemical detection of miR-21 in gastric cancer patients. T4 RNA ligase 2 catalyzes a particular reaction between the DNA probe (DNA2) and the target RNA, hybridizing to DNA1. To amplify the response signal, a two-stage CEAM was conducted: (i) T7 exonuclease digested DNA1 and (ii) T7 exonuclease digested the DNA3 probe and hybridized with DNA1 from the previous stage. The remaining DNA3 sequences, tagged with thiol group and Fc, were immobilized on an AuNP-modified electrode, generating a voltammetric signal response. Higher concentrations of miR-21 in the reaction mixture resulted in lower DNA3 digestion and, therefore, more DNA3 probes were immobilized on the electrodes. Using this amplification strategy in combination with the AuNP-electrode, an LOD of 0.36 fM with high specificity was obtained.[80]

Tao et al. introduced an electrochemical miRNA biosensing system by combining a double-loop hairpin probe (DHP) and doxorubicin-functionalized AuNPs (AuNPs@Dox) to detect miRNA let-7d. DHP comprised a sequence for target miRNA hybridization, an output part, and a complementary sequence for the output segment. Upon the hybridization of the target RNA with DHP, DNA–miRNA heteroduplexes were formed. Using DSN, the DNA in the heteroduplex was hydrolyzed, releasing the output segment and the target miRNA and, thus, a new cycle. The biosensor was assembled by immobilizing the DNA probes (DNA S1) conjugated with AuNPs@Dox (AuNPs@Dox@S1) on an Au electrode to amplify the electrochemical signal as well as the sensitivity. By hybridizing with the let-7d, the released output segments were displaced with the AuNPs@Dox@S1 probes, functionalized the Au electrode surface, and reduced the current. The proposed platform had 0.17 pM LOD and a wide dynamic range from 0.1 pM to 10 nM.[81]

DNA hydrogels for the signal amplification approach have also recently gained much attention. These porous 3D network polymers constitute high amounts of water formed by cross-linking nucleic acid-tethered polymer chains.[82] Recently, Deng's group introduced an in situ terminus-regulated DNA hydrogelation approach coupled with an miRNA electrochemical microarray. The target miRNA was captured by the hairpin probes fixed on the Au electrodes, leading to their opening. The result from the exposed 3′-OH end was then tailed by the TdT-mobilized feeds of dATP and branched using the oligo T20G5. The isothermal amplification of dendritic DNA was followed by its gelatinization into an intricate 3D network (Fig. 6A). The electrochemical response was due to the streptavidin–HRP conjugates. Using the platform for the hsa-let-7d-5p model target, an LOD of 0.35 fM and a dynamic range of 1 fM to 10 pM were achieved.[83]

Zhang et al. used a triple signal increase strategy to develop an electrochemical detection system for miR-21. They combined a DSN-assisted target recycling, which used AuNPs and HRP enzymes. Following the addition of the sample, the target miRNAs hybridized with the hairpin DNA probes residing on the gold electrode, forming DNA/RNA duplexes. After that, the duplexes were cleaved selectively by DSN, which triggered the discharge and recycling of the target miRNAs. The residual DNA segment was then hybridized with the biotinylated signal DNAs (sDNAs), leading to the capture of streptavidin-coated AuNPs and the capture of the biotin-labeled HRPs. The AuNPs enhanced the electron transfer from HRPs to the gold electrode. This nanobiosensor showed a dynamic range from 0.1 fM to 100 pM and an LOD equal to 43.3 aM.[84]

Most electrochemical miRNA biosensors are time-consuming and complex, require multiple reagents, have low applicability for miRNA detection in complex samples, and require different amplification strategies.[85] Zouari et al. reported an RNA/RNA hybridization assay to overcome these shortcomings, wherein the target miRNAs competed with synthetic biotinylated miRNAs to be hybridized with the thiolated complementary probes immobilized on an AuNPs-modified electrode. The

Fig. 6 Electrochemical sensors for ultra-sensitive miRNA detection. (A) DNA hydrogels on gold electrodes[83] and (B) using barcode gold nanoflowers.[88]

amperometric response was generated *via* the labeling of the hybridization of the biotinylated miRNA with streptavidin-modified HRP, followed by the addition of H_2O_2/hydro-quinone. This diagnostic system successfully detected the model target miRNA-21 from 100 fM to 25.0 pM within 75 min. A very low detection limit (25 fM) with remarkable

selectivity, even in single mismatch differentiation, was obtained without any amplification step. The system was further applied to determine the miRNA levels in total RNA extracted from both tumor and healthy cells.[85]

Most electrochemical sensors developed for miRNA detection include labeling procedures using redox enzymes, electrocatalytic molecules, or electro-active nanotags. Designing label-free and reagent-less electrochemical systems has been a challenge. Tran et al. described a reagent-less and label-free miRNA biosensor using a self-assembled monolayer (SAM) comprising a mixture of 4-naphthoquinone (JUG-SH), 5-hydroxy-3-hexanedithiol-1, and 6-mercaptohexanoic acid (6-MHA) on an AuNPs-modified GCE (AuNPs/GCE). Herein, 6-MHA was applied as an attaching site for immobilizing NH_2-modified DNA probes, whereas JUG-SH was used as a transducing element to probe the biomolecular interactions. An increase in the current was recorded after the hybridization of the target at the SAM/solution interface. The resulting biosensor could detect down to 100 fM target miRNA and had a dynamic range from 100 fM to 5 nM.[86] The application of AuNPs/GCE in electrochemical miRNA biosensors was also reported in 2016, wherein a detection strategy based on DNAzyme-based target recycling amplification combined with porous palladium-functionalized HRP (Pd@HRP) was developed. The proposed electrochemical biosensor achieved an LOD of 0.2 fM and had a broad dynamic range of 3 fM–1 nM.[87]

Recently, Mohammadniaei and coworkers reported a detection system using barcode gold nanoflowers for ultra-sensitive miR-21 detection. They designed a three-way junction RNA with a hairpin structure, which unfolded in the occurrence of miR-21. The hybridization of the target miRNA followed this with the sensing moiety of the RNA probe and, afterward, its attachment to the gold nanoflower/platinum electrode (GNF@Pt) coated with DNA. Subsequently, the barcode-AuNPs (MB/barG) were added and captured by the other two legs of the RNA probe (Fig. 6B). The biosensor required small amounts of sample (4 μL), had a sensitivity as low as 135 aM or 324 molecules, and operated within the range of 1 μM to 500 aM. The use of MB/barGs showed an excellent influence on the final signal by 230 times amplification.[88]

In another attempt, using an Au-paper working electrode (Au-PWE) increased the surface area for the recognition elements. In this regard, the authors designed a paper-based biosensing system for the ultra-sensitive detection of miRNAs. They modified the paper electrode with AuNPs to promote conductivity and immobilize hairpin probes (H1). When target miRNAs are present, the opening and hybridization of H1 hairpins are started. Following the addition of a second hairpin probe (H2), due to its higher hybridizing affinity capacity with H1 compared to the miR-155, the target was released, and a new cycle was started. Subsequently, the exposed portion of the H1–H2 duplex captured the AuNPs–Cu metal–organic frameworks harboring many DNA strands (S1-AuNPs@Cu-MOFs). The electrochemical response was generated through glucose oxidation by Cu-MOFs, resulting in a low LOD of 0.35 fM and also a wide linear range.[63]

Su et al. showed that multilayered nanoprobes could amplify the signal in miRNA detection. Their work developed a sandwich electrochemical assay using MoS_2–AuNPs-based multilayered nanoprobes designed with DNA probes. Two thiolated ssDNA probes, probe 1 and probe 2, were assembled on each of the MoS_2–AuNPs (SLNPs). After that, the two MoS_2–AuNPs-based nanoprobes were hybridized with each other, producing a multilayered nanoprobe. The MLNPs were then stabilized using another thiolated DNA. After adding miRNA-21, electrostatic repulsion was formed between DNA4 and the $[Fe(CN)_6]^{3-/4-}$ ion. The MCH blocked the active sites on the Au surface, preventing any unwanted connections. In the presence of a target analyte, a sandwich structure occurs between the MCH/DNA4/Au and MLNPs, altering the impedance of MLNPs and MCH/DNA4/Au. The EIS-based biosensor demonstrated a dynamic range from 10 aM to 1 μM and an LOD of 38 aM for miRNA-21 in cervical cancer cells.[89]

Sabahi et al. described an electrochemical biosensor by measuring the Cd^{2+} amplification signal for detecting miRNA-21. High specificity and sensitivity were obtained by combining two nanomaterials. This biosensor placed single-wall carbon nanotubes (SWCNTs) on the fluorine-doped tin oxide (FTO) electrode. Dendritic gold nanostructures were used to immobilize the thiolated receptor probe coupled with SWCNTs through a single-layer self-assembly to customize the biosensor. 11-Mercapto-1-undecanol (MU) blocked all the empty spaces, arranging the connected miRNA-21 receiver probes. An electrostatic connection between Cd^{2+} and miRNA-21 turned Cd^{2+}-labelled miRNA-21 into a signal amplifier and was eventually hybridized with the PNA probe. Cadmium oxidation was measured in the presence of miRNA-21. This point-of-care DPV biosensor obtained an LOD of 0.01 fM with a broad dynamic range from 0.01 fM to 1 μM.[90]

An electrochemical miRNA biosensor with a base stacking effect and a novel sandwich pattern was developed. Gold nanostructures were decorated and grown on SPCE, forming gold nanostructures with high curvature. A short (10 nucleotides) DNA capture probe (CP) was then self-assembled with Au–S bonds. In the presence of miRNA, blending biotinylated stacking probe (SP) and miRNA provided a duplex miRNA-SP structure combined with DNA target via base-stacking through sandwich formation. The gold pattern on the electrode determined the miRNA-SP/CP connections at different angles, increasing the connection probability. The ultrasensitive sensor detected miRNA-21 with different sequences and structures (Fig. 7A). The reported LOD was 7.5 fM, and the linear range was from 10 fM to 1 nM.[91]

miRNA-410 is one of the most important biomarkers for diagnosing prostate cancer. Yaman et al. studied a graphite electrode modified with peptide nanotubes-decorated AuNPs (AuNP–PNT). In order to be specific, DNA probes were covalently bonded to AuNP/PNT. The dynamic range and LOD were in the range from 10 fM to 300 pM and 3.90 fM, respectively. This inexpensive electrochemical provided a low LOD, high selectivity, high stability, and rapid detection process.[92]

Fig. 7 Electrochemical sensor (A) based on gold nanostructures modified with a short DNA probe for miR21 detection.[91] (B) Open-channel mini-pillar biosensor for detecting multiple Alzheimer's biomarkers.[94]

In another miR-21 detection technology, the MB redox reaction with new signal amplification materials was used. This sensor attached polypyrrole (PPY) and graphene (GP) to an SPCE as an amplifier composite. A mixture of AuNPs and DNA-21 probes was conjugated to the GP/PPY composite, whereas the empty areas were blocked using MCH. Two signals corresponding with MB, and with and without miRNA, were observed in DPV. In the presence of miRNA, the duplex DNA/miRNA was formed, whereas in its absence, MB was absorbed, and different signals against the captured DNA/MB were created. This biosensor had a dynamic range between 1.0 fM and 1.0 nM, and the LOD was 0.020 fM with high sensitivity, stability, repeatability, and specificity.[93]

Song *et al.* prepared a novel multifunctional electro-chemical microreactor for the concurrent tracing of Alzheimer's biomarker miRNA-101. This open channel sensor contained two main parts: an integrated circuit board and a minipillar platform. In the mini pillar, polydimethylsiloxane was used as the absorbent agent. In the three-electrode array, gold nanodendrites acted as the working, silver as the reference, and platinum as the counter electrode. DNA hairpin probes were functionalized on the electrode during redox and were hybridized to miRNA-101 with high selectivity and speci-

ficity. Establishing the connection in different doping altered the SWV response (Fig. 7B). This sensor had a fine dynamic range of 10^{-10} to 10^{-7} M and an LOD of 91.4 pM.[94]

In a study by Daneshpour *et al.*, an miRNA nanobiosensor was fabricated using gold-magnetic nanostructures on modified screen-printed electrodes. These nanostructures were decorated with ssDNA probe 1, and their magnetic properties played a crucial role in target separation in the sample solution.[95] The second ssDNA probes were immobilized on the electrode and acted as a capture probe, forming a sandwich hybrid with target miRNA and probe 1. The hybrid was made with the target miRNA, generating a measurable signal due to the electrochemical properties of the gold nanocomposites. This nanobiosensor showed an acceptable linear range from 1 $\times 10^{-3}$ pM to 1×10^3 pM and an LOD of 3×10^{-4} pM. Later, the authors upgraded their system into a dual signal nanobiosensor to simultaneously detect two miRNAs (an oncogenic and a tumor suppressor) associated with gastric cancer (GC). Thanks to the magnetic nanocomposites containing Au NPs and CdSe@CdS quantum dots (as the electrochemical labels) and a mixture of polythiophene/rGO on the carbon electrodes, this nanobiosensor reached a remarkable analytical performance in the evaluation of miR-106a and let-7a. The results revealed that modifying the electrode surface with conductive materials considerably improved the biosensing performance. The nanobiosensor had very low LODs of 0.02 fM (let-7a) and 0.06 fM (miR-106a) and thus could be applied in the early diagnosis of GC and screening different miRNA sequences.[96]

The use of gold nanoparticles (AuNPs) in developing miRNA biosensors is undoubtedly a remarkable breakthrough that offers a multitude of advantages. They enhance the sensitivity, contributing to the accurate detection of miRNAs. Their easy functionalization allows for the tailored design and modification of capture probes, leading to specific binding with target miRNAs. This specificity reduces the likelihood of false-positive results, making AuNPs a reliable choice for miRNA biosensing applications. Furthermore, their catalytic activity can be harnessed to amplify signals, improving the overall per-

formance of biosensors.[97–99] Despite their advantages, AuNPs have certain limitations. The primary concern is their relatively high cost, which can restrict the scalability of miRNA biosensor production. Additionally, variations in the size and shape of AuNPs can affect their performance, necessitating precise control over these parameters. Moreover, there are potential concerns regarding the long-term stability of AuNPs in biosensors and their possible toxicity. Another issue to consider is the propensity of AuNPs to accumulate on the sensing electrodes, which can lead to false-positive results in miRNA biosensing.[100–102]

2.2.2. Silver nanoparticles and composites. Silver nanoparticles (AgNPs) are another common metal particle in sensing applications. They are considered effective electrocatalysts, especially in the oxidation process of electrochemical sensors. By controlling the size and shape of AgNPs, they can help with label-free detection and more sensitive and amplified responses to various novel electrochemical sensing platforms.[103,104] The miRNA sensors developed based on this technology are reviewed in Table 5. In 2018, Gao *et al.* constructed a novel electrochemical nanobiosensor to simultaneously determine miR-16 and alpha-fetoprotein (AFP) as hepatocellular carcinoma (HCC) diagnostic biomarkers. The authors reported the design of a dual-aptamer hairpin consisting of miR-16 complementary and AFP aptamer sequences as the sensing probe. The probe was labeled with a thiol group and MB in its 3′ and 5′ terminals, respectively, and was immobilized on the Au electrode surface through Au–thiol bonds. In the absence of the target, a relatively large electrochemical signal was detected because of the closeness of tangled MB into the hairpin DNA and Au electrode surface. After adding an miR-16 and AFP mixed solution on the sensing probe-modified Au electrode surface, the fixed sensing probe simultaneously captured the two targets. The hairpin opened when the sensing probe was hybridized with miR-16, and the MB-related electrochemical signal showed considerable attenuation. For the AFP assay, concanavalin A (ConA)-modified AgNPs, used as the signal detector, bonded to the

Table 5 Electrochemical sensors based on silver nanoparticles for miRNA detection

miRNA	Nanoparticles and other electrode modifications	Electrochemical method	Linear range	Detection limit	Ref.
miR-21	AgNPs as detector	LSV	0.1 fM–2 pM	20 aM	107
miR-25	Cys–AuNPs as platform	DPV	10^{-12} to 10^{-10} M	3.13×10^{-13} M	108
	AgNPs/SWCNTs as detector		10^{-10} to 10^{-8} M		
miR-16	AgNPs	DPV	50–2000 nM	0.14 nM	105
miRNA-21	AgNF	CV	2×10^{-16} to 1×10^{-9} M	0.20 fM	109
miR-141, miR-21	AgNWs/AuNPs as platform and PtCu as detector	SWV	10^{-15} to 10^{-9} M	0.1 fM	106
miR-7a	AuNPs catalyzing Ag clusters	DPV	50 fM–250 pM	15 fM	110
miR-9-2	Ag–Au mesoporous alloy film	DPV	100 pM–100 aM	100 aM	111
miR-21	AgNPs	SWV	1 fM–200 pM	0.4 fM	112
miR-155	PEI–AgNPs	CV	20 zmol–2 pmol	20 zmol	113
Model miRNA	DNA-functionalized AuNPs–AgNPs	LSV	1 fM–1 pM	0.62 fM	114

AuNWs: gold nanowire, rGO: reduced graphene oxide DPV: differential pulse voltammetry, CV: cyclic voltammetry, LSV: linear-sweep voltammetry, AgNPs: silver nanoparticles, Au NPs: gold nanoparticles, SWCNTs: single-walled carbon nanotubes, AFP: alpha-fetoprotein, AgNF: silver nanofoam, AgNWs: silver nanowires, SWV: square wave voltammetry, AuAgNR: gold and silver nanorod.

captured AFP *via* the glycosidic bond, generating a detection signal. MB and AgNPs did not interfere with each other and enabled a one-step detection for both the targets. The nanobiosensor showed a linear range from 50 to 2000 nM and an LOD of 0.14 nM for miR-16. A wide dynamic range from 50 pg mL^{-1} to 10 ng mL^{-1} and an LOD of 8.76 pg mL^{-1} were reported for AFP. Compared with traditional single/multiplex detection strategies, the biosensing system improved the sensitivity and selectivity for the clinical detection of HCC.[105]

Tian *et al.* designed a paper-based electrochemical nanobiosensor using MOF as well as hierarchically assembled nanomaterials to detect miR-141 and miR-21 simultaneously. The silver nanowire (AgNW) film supported the electrode's conductivity. Then, the AgNW-modified electrode was decorated with a 2D composite of molybdenum sulfide (MoS$_2$)/AuNPs to provide a larger active surface area for the capture probes, resulting in higher electrochemical currents. In the next step, the hairpin probes (DNA1 and DNA2; complementary for miR-141 and miR-21, respectively) were functionalized on the AgNWs/MoS$_2$/AuNPs-based electrode. The sample was then added, followed by inserting the PtCuMOFs/DNA3/MB/Fc and PtCuMOFs/DNA4/MB/Fc into the reaction spot. PtCuMOFs are electrochemical activator molecules that act as a carrier for capturing detector probes and DNA3 and DNA4 that were applied as detector probes in SWV analysis. Under optimal conditions, the paper-based electrochemical sensor demonstrated an LOD of 0.1 fM to detect the miR-141 and miR-21 simultaneously. Therefore, the dual detection strategy was considered to be suitable for diagnosing different cancers.[106]

Liu *et al.* developed a sensitive and label-free electrochemical miRNA nanobiosensor using the *in situ* aggregation of silver nanoparticles. The hairpin-like DNA stem-loop structure with a thiol modification at the 5′-end was used as a biocomponent restrained on the nano-Au electrode surface using the Au–S bonds. After adding the target miRNAs, the hairpin structure opened due to the hybridization reaction, and miRNA-21 was anchored on the electrode surface. Then, 4-mercapto phenylboronic acid (MPBA) and citrate-capped AgNPs were deposited on the Au electrode. The boronate ester bonds resulted from the reaction between *cis*-diol on the 3′-end of the anchored miRNA-21 ribose and MPBA. In the biosensing system, MPBA operated as a cross-linker for AgNP assembly and induced the accumulation of citrate-capped AgNPs *via* sulfide bonds. The aggregated AgNPs acted as a label for the molecular recognition of the target. Using linear-sweep voltammetry (LSV), the detection range and LOD were reported to be 0.1 fM to 2 pM and 20 aM, respectively. The biosensor has shown promising potential for direct and sensitive miRNA detection with no need of functionalization of nanoparticles or labeling the capture/detection probes.[107]

A significant increase in miR-25 expression in lung cancer is associated with tumorigenesis; it is, thus, a suitable biomarker for lung cancer detection. Using a nanohybrid structure composed of AgNPs with single-walled carbon nanotubes (SWCNTs), Asadzadeh-Firouzabadi and her coworker designed a novel electrochemical genosensor for sensitive miR-25 detec-

tion. AgNPs and SWCNTs in the nanohybrid structure were responsible for interacting with the probe and producing electroanalytical signals, respectively. The GCE surface was modified using Cys–AuNPs *via* the interaction of the electrode with the amine linker of Cys–AuNPs. After adding glutaraldehyde (GA) followed by the attachment of the NH$_2$-probe to the surface of the electrode, the sample was placed on the probe/GA/Cys–AuNPs-modified GCE. Finally, the AgNPs/SWCNTs were absorbed on the surface. Due to the bases being shielded inside the double helix, the binding forces formed between AgNPs/SWCNT nanocomposites, and the nitrogenous bases were less strong than those of single-stranded nucleic acid. The final detection using DPV analysis was based on AgNPs-loaded SWCNTs oxidation as the label. The amplification-free nanogenosensor was applied to detect miR-25 as the analyte in two linear concentration ranges, 1.0×10^{-12} to 1.0×10^{-10} M and 1.0×10^{-10} to 1.0×10^{-8} M with an LOD of 3.13×10^{-13} M. Taking advantage of AgNPs/SWCNTs nanocomposite for binding to the single-stranded probe, the proposed biosensor facilitated the recognition and quantification of miRNAs solely by redesigning the probes.[108]

Kangkamano *et al.* fabricated a label-free voltammetric nanogenosensor using polypyrrole (Ppy) and silver nanofoam (AgNF) for miR-21 detection. The gold electrode was first coated with electrodeposited AgNF, followed by the electropolymerization of the PPy conductive polymer to facilitate the immobilization of the pyrrolidinyl peptide nucleic acid probes.[65] After the hybridization of the PNA probes and the target miRNA, some low current redox peaks were recorded due to the obstructed charge transfer from the electrolyte to the electrode. The suggested nanogenosensor displayed a linear range, LOD, and analysis time of 2.0×10^{-16} M to 1.0×10^{-9} M, 0.20 fM, and 5 min, respectively. Using real samples (recoveries 81–119%), the label-free electrochemical PNA biosensor was shown to analyze miRNA-21 or other miRNAs without needing RNA extraction and amplification.[109]

A sensitive biosensor for miR-7a detection was suggested by Wen *et al.* The electrochemical platform consisted of two nano parts (probes): first, the magnetic beads were coated with captured probes, and AuNPs were functionalized with reporter probes. These two probes with complementary sequences for miR-7a formed a sandwich assay. With target miR-7a, a sandwich was formed, and by adding silver salt and reducing agents, Ag clusters were synthesized around the AuNPs. Afterward, the complexes mentioned above were separated using magnetic beads. After adding HNO$_3$, Ag atoms were precipitated, and the electrochemical output signal was measured using DPV. The sensor showed a linear range between 50 fM and 250 pM with an LOD of 15 fM. The high sensitivity and accuracy of the platform were due to the use of multiple signal enhancement strategies. The 70-minute response time was one of the main limitations of the sensor.[110]

miR-9-2, as the biomarker of metastatic nasopharyngeal carcinoma, was detected by Park *et al.* The Ag–Au mesoporous film was prepared electrochemically. Polymeric micelles were used to create pores in the film. This bimetallic film provided

a greater surface for electrochemical oxidoreductive properties of potassium ferro/ferricyanide complex ($[Fe(CN)_6]^{3-/4-}$) during DPV measurements. Firstly, the sample was purified using a biotinylated complementary sequence for miR-9-2 and magnetic beads. Then, the Ag–Au alloy film was exposed to the purified miRNAs, and the electrochemical signals were generated. This platform represented a cost-effective method because of being amplification and enzyme-free. The electrochemical synthesis of the Ag–Au mesoporous film was highly reproducible. The linear range of the sensor and its LOD were 100 pM to 100 aM and 100 aM, respectively.[111]

Cheng *et al.* used a two-signal amplification method to detect exosomal RNAs like miR-21. The first hairpin sequence complementary to miR-21 was fixed on the gold electrode and then bonded to miR-21. Later, the second hairpin (complementary to the first hairpin) was added to help separate miR-21 by attaching it to the first hairpin. The released miR-21 then bonded to the fixed hairpins, thus enhancing the final signal. Second hairpins, being biotinylated, attached to streptavidin–AgNPs that were also attached to the biotinylated AgNPs, again helping with signal enhancement (Fig. 8A). The as-described enzyme-free sensor had a low LOD (0.4 fM), good selectivity, and low cost. Its linear range was between 1 fM and 200 pM.[112]

A highly sensitive electrochemical sensor was reported by Hakimian *et al.* for the detection of miR-155. The miR-155 complementary hairpins were immobilized on the gold surface. With the target miR-155, the hairpins opened, and the positively charged polyethene imine silver nanoparticles (PEI–AgNPs) electrostatically bonded to the negatively charged oligonucleotides. This phenomenon helped create great anionic CV peaks and thus led to high sensor sensitivity. The linear range and the nanobiosensor's LOD were 20 zmol to 2 pmol and 20 zmol, respectively. The platform was fast, cost-effective, simple, and sensitive.[113]

Wang *et al.* developed a miRNA sensing in which the citrate-capped AuNPs were electrostatically functionalized using DNA probes. These DNA-functionalized AuNPs attached to the GCE surface and hindered the attachment of AgNPs to the electrode due to steric and electrostatic repulsions. Without the target miRNA, a low signal was observed. In its presence, however, miRNA bonded to DNAs and was digested by duplex-specific nuclease (DSN). Following the hinderance removal by DNA/miRNA enzymatic digestion, Au and Ag NPs accumulated on the electrode, generating sharp LSV signals. Despite advantages such as high selectivity and sensitivity, the platform was time-consuming and expensive due to the need for enzymes (Fig. 8B). The sensor was linear in the 1 fM–1 pM range, with an LOD of 0.62 pM.[114]

Despite being economical compared with their gold counterparts, the usage of silver nanoparticles in the design of electrochemical nanobiosensors is still limited since the cost difference has not been able to offset the preference for the unique properties of AuNPs. In addition, there is evidence that chronic exposure to Ag is linked with various health problems. Due to the size and possible deeper penetration, Ag nano-

materials have shown higher levels of toxic effects on the environment and human health, which may raise concerns about using them in biomedical devices.[115] In conclusion, AgNPs contribute to enhanced sensitivity through catalytic activity and large surface areas. Nevertheless, potential toxicity is a concern, and stability in various environments may be challenging.

2.2.3. Magnetic and other metal nanoparticles. Magnetic nanoparticles are one of the other promising NPs used in the electrochemical detection of therapeutic miRNAs. They are used as transducers or for sample preparation steps. Apart from being non-toxic, easy to prepare, and biocompatible, they can help improve sensitivity and selectivity in electrochemical sensors.[116,117] Table 6 represents several sensors developed using these nanoparticles.

Zhou *et al.* developed a nanobiosensor for miRNA-155 detection *via* dual electrochemical–optical methodology. A paper-based electrode was modified with AuNPs and bonded with the first hairpin (H1) *via* Au–S bonds to form the detection layer. With the target miR-155, H1 was opened and attached to the second hairpin (H2). The CuCo–CeO$_2$ nanospheres were then immobilized on H2 using a short complementary sequence (called S1). Then, H$_2$O$_2$ was decomposed due to its catalytic properties, generating an electrochemical response. The LOD and linear range of the nanobiosensor were reported to be 0.05 fM and 0.1 fM to 10 nM, respectively. It could also provide a sensitive colored response based on 3,3′,5,5′-tetramethylbenzidine (TMB) oxidation in real serum samples.[118]

A sensitive and accurate sensor was introduced by Yu *et al.* In this platform, MNPs were decorated with AuNPs and coated with probes complementary to the target miRNA (probe A). According to the isothermal duplex-specific nuclease (DSN) properties, the double-stranded miRNA-probe A structures were cleaved, and uncleaved probes were magnetically separated. On the other hand, probe B was tagged with TCEP (active electrochemical molecule) and immobilized on the electrode surface. As a result, a strong signal was recorded in the absence of the target miRNA while in its presence, probe A-miRNA was cleaved, and the released probe, along with the two others already existing in the system (probe C and probe D), were attached to probe B to form a four-junction DNA structure. The endonuclease later disrupted the DNA structure, and the TCEP molecules were then separated and washed out. The higher concentration of miRNA in the sample resulted in a higher decrease in the SWV peak current. The calculated LOD was 3 aM, and the linear range was from 10 aM to 10 fM. The low LOD, high accuracy, and sensitivity of the sensor are due to the use of a combination of three different signal amplification methods: DSN, nicking endonuclease, and TCEPs.[119]

In a nanobiosensor presented by Jia *et al.*, β-FeOOH nanorods (NRs) were decorated with polyoxometalate-derived MoS$_2$ nanosheets (pd-MoS$_2$ NSs), providing an opportunity for high-affinity binding to cDNA and also good electrochemical performance. cDNA was then immobilized on the electrode surface, already modified with the as-described nano-

Fig. 8 The schematic illustrations of electrochemical sensors (A) based on silver nanoparticles for miRNA-21 detection[112] and (B) based on the co-decoration of Au and AgNPs on glassy carbon electrode for miRNA detection.[114]

composite. In the presence of the target, the miRNA attached to the immobilized cDNA changes the EIS electrochemical response. The reported range was from 1 fM to 5 nM with an LOD of 0.11 fM. High selectivity, reproducibility, and stability were the main advantages of the sensor, besides its being simple.[120]

In another biosensor for miRNA-21 detection, the Fe–N–C nanocomposite was functionalized with thionine and then decorated with Fe_3O_4@AuNPs. It was then attached to a magnetic glassy carbon electrode (MGCE) *via* electromagnetic forces. The target miRNA-21 matched with a hairpin (H1) and afterward replaced with the second hairpin (H2) tagged with SiO_2 nanoparticles following a catalytic hairpin assembly (CHA) reaction. Afterward, the H1/H2 nucleic acid structure attached to the Fe–N–C/thionine and Fe_3O_4@AuNPs over the electrode and robust DPV electrochemical responses were

Table 6 Magnetic nanoparticle-based electrochemical sensors for miRNA detection

miRNA	Nanoparticles and other electrode modifications	Electrochemical method	Linear range	Detection limit	Ref.
miR-155	CuCo–CeO$_2$ nanospheres, Au-modified paper electrode	DPV	0.1 fM–10 nM	0.05 fM	118
Model miRNA	MNPs@AuNPs, DNA four-junction	SWV	10 aM–10 fM	3 aM	119
miR-21	pd-MoS$_2$ NSs, β-FeOOH nanorods (NRs)	EIS	1 fM–5 nM	0.11 fM	120
miR-21	Fe–N–C–thionine, Fe$_3$O$_4$@AuNPs, MGCE	DPV	1 fM–10 nM	0.63 fM	121
miR-21	MNPs, PtNPs	Current changes	50 aM–5 nM	47 aM	122
miR-9-2	Mesoporous gold electrode, magnetic beads	DPV	100 aM–1 nM	100 aM	123
miR-21	Magnetic beads, gold electrode, G-quadruplex DNA structure	DPV	10 fM–10 nM	2.75 fM	125
miR-21	Magnetic beads, AuNRs, AuNF-modified ITO electrode	DPV	1 aM–1 nM	0.32 aM	127
miR-21	Nickel phosphate flower-shaped nanostructure	EIS	0.1–2500 pM	0.034 pM	128
miR-155	Fe$_3$O$_4$NPs@Ag core–shell nanoparticles	DPV	0.5 fM–1.0 nM	0.15 fM	129

SWV: square wave voltammetry, AuNPs: gold nanoparticles, MNP: magnetic nanoparticles, MGCE: magnetic glassy carbon electrode, PtNPs: platinum nanoparticles, AuNRs: gold nanorods, AuNF: gold nanoflower.

recorded. The LOD and dynamic range were 0.63 fM and 1 fM to 10 nM, respectively. The sensor had high sensitivity and reproducibility and worked under different pH conditions as well as in real serum samples.[121]

Bai *et al.* developed a single-entity electrochemical biosensor (SEECBS) consisting of magnetic nanoparticles altered with satellite MNPs by attaching PtNPs to their surface through ssDNA linkers. miRNA-21 attached to the linker ssDNA, forming a double-stranded moiety cleaved by duplex-specific nuclease (DSN). After cleavage, the non-reacted ssDNAs attached to the MNPs–PtNPs satellite were eliminated from the reaction chamber by the magnetic field. At the same time, the electrode was exposed to the other reagents. Due to their electroactive catalytic properties, ptNPs (released after cleavage) generated current, producing a good detection window with an LOD of 47 aM and linearity from 50 aM to 5 nM. The new sensor detected attomolar concentrations of miRNA-21 in the MCF-7 cell culture.[122]

A mesoporous gold electrode-based portable biosensor was studied by Masud *et al.* Target miRNA 9-2 was extracted from the exosomes and further purified and concentrated using magnetic nanobeads, already coated with specific probes for the target miRNA. After separating miRNA 9-2 from the magnetic beads (by heat release), the miRNAs were adsorbed on the mesoporous gold electrode. The DPV electrochemical response was generated based on the reduction activity of [Fe(CN)$_6$]$^{3-/4-}$ ions. The more miRNAs bonded to the electrode, the higher the DPV reduction signals recorded. The easy-to-fabricate sensor was linear between 100 aM to 1 nM and had an LOD of 100 aM.[123]

Tang *et al.* fabricated an miRNA-21 sensor for breast cancer diagnosis. Firstly, the exosomes were sampled from human serum, and miRNA-21 was purified using specific magnetic beads coated with locked nucleic acid (LNA)-modified DNA probe1 bonded to probe 2. In the presence of the analyte, it was replaced with probe 2 and was washed out from future reactions using the magnetic beads. The released probe 2 triggered a rolling circle amplification[124] and produced several G-rich DNA structures, called G-quadruplex, with embedded MB electrochemical active molecules in their structure to generate robust signals. The sensor showed an LOD and linearity of 2.75 fM and 10 fM–10 nM, respectively.[125]

Another miR-21 nanobiosensor was reported by Peng *et al.* In this sensor, magnetic beads were coated with H1 (hairpin 1) were complemented with miRNA-21. After that, H2 attached to AuNPs was replaced with miRNA-21 through a strand displacement amplification.[126] The miRNAs were then released to trigger the binding of the magnetic beads/H1 and AuNRs/H2, developing a network-like structure. Afterward, propargyl-2-bromoisobutyrate (PBIB) molecules were attached to the 3′ end on H2 to start atom transfer radical polymerization (eATRP) after the addition of ferrocenylmethyl methacrylate (FMMA) monomers. PBIB worked as the polymerization initiator. Besides being electroactive, eATRP and SDA amplified the final signal about 35 times. A low LOD (0.32 aM) and linear range between 1 aM and 1 nM were obtained (Fig. 9A). In this system, the ITO electrode was modified with gold nanoflowers (AuNF) for more sensitive results.[127]

Kannan *et al.* developed a sensor for miRNA-21 detection using modified GCE. A flower-like nickel phosphate nanostructure (NiPN) was synthesized and attached to the electrode surface, and miRNA-21 complementary probes were immobilized on the NiPN structure. The more target the miRNA was attached to the modified GCE, the higher the recorded resistance (Fig. 9B). The reported LOD was 0.034 pM, and the sensor had two linearities between 0.1 and 2500 pM. Its simplicity and efficiency made the platform suitable for rapid point-of-care applications.[128]

As for miRNA-155, a novel biosensor was suggested by Yazdanparast *et al.* In this sensor, magnetic core–shell Fe$_3$O$_4$@Ag nanoparticles functionalized with ssDNA complementary to miRNA-155 were attached to a carbon paste electrode containing a magnetic bar (MBCPE). After adding resveratrol (RSV) as an electroactive molecule, an oxidation peak was recorded in DPV analysis, and RSV has a higher affinity to dsDNA than ssDNA. In the presence of miRNA-155, a double-stranded structure was formed between the miRNA and capture probe, attracting more RSVs and thus resulting in higher signals (Fig. 9C). The LOD and linear range were reported to be 0.15 fM and 0.5 fM–1.0 nM, respectively. The

Fig. 9 (A) Two amplified sensors using SDA and eATRP for miRNA-21 detection,[127] (B) nickel phosphate flower-shaped nanostructure-modified GCE for miRNA detection,[128] and (C) core−shell Fe₃O₄@Ag nanoparticles for miRNA-155 detection.[129]

sensor had good reproducibility and specificity in assessing real serum samples.[129]

Magnetic nanoparticles are valuable components in miRNA biosensors, offering significant advantages. Their magnetic properties facilitate the easy separation and concentration of target miRNAs, particularly in complex sample matrices, enhancing the overall sensitivity.[130] Moreover, some magnetic nanoparticles exhibit biocompatibility and low cytotoxicity, making them suitable for biological applications.[131] However, challenges may arise regarding their potential susceptibility to

agglomeration, which requires careful dispersion management.[132] Overall, the benefits of magnetic nanoparticles in miRNA biosensors include efficient target isolation, but effective dispersion and tailored selection are crucial to address potential limitations.

2.2.4. Novel metal–organic and inorganic complex nanostructures

2.2.4.1. Metal–organic framework (MOF). MOFs are a kind of porous material consisting of organic linkers and metal nodes. They have special physical, electrical, and conductive behaviors. Their highly ordered crystalline nature of MOFs and high stability and porosity have made them good candidates for electrocatalytic applications. Different functionalization processes and structures have turned them into next-generation materials in electrochemical sensing.[133] They are mainly used in combination with other nanomaterials for better attachment to the electrode surface. In electrochemical sensors, high oxidation-state MOFs are more advantageous.[134] The list of MOFs used for different biosensor applications is growing; in Table 7, however, we have only listed MOFs-based nanobiosensors for miRNA detection.

Li *et al.* fabricated an electrochemical nanobiosensor based on the catalytic properties of a layered MOF (MIL-88@Pt@MIL-88) for miRNA-21 detection. A capture probe was decorated on the gold electrode (GE), where a protector probe was attached to prevent the layered MOF@Pt@MOF/signal probe from binding to the capture probe. Exposing to miRNA-21, a primer exchange reaction (PER) started by a hairpin already existed in the test chamber. It produced a PER product, a long oligonucleotide with multiple attachment sites for the protector probe. This helped detach the protector from the capture probe, allowing the MOF@Pt@MOF/signal probe to bind with the electrode. Due to its peroxidase-like properties, MOF@Pt@MOF converted H_2O_2 into H_2O and O_2, generating DPV signals. This sensor was linear between 1 fM and 1 nM, had an LOD of 0.29 fM, and had good selectivity when used with real samples. The low-cost system helped with the enzymatic activities, making it more interesting for scientists trying to make affordable enzyme-based nanobiosensors.[135]

Meng *et al.* presented an miRNA nanobiosensor based on immobilizing hairpin capture probes (HP1) on the gold electrode surface (GE). The HP1 is linked with the target miRNA, becoming linear in structure. Then, Pd@MOF (Pd@UiO-66), attached to another hairpin (HP2), was exchanged with the miRNA-21 and bonded to the HP1. miRNA-21 was then recycled to improve the Pd@MOF attachment on the GE. Considering the catalytic properties of Pd@MOF, paracetamol (AP) electroactive molecules were added to generate the DPV electrochemical signals in the presence of miRNA-21 (Fig. 10A). The linear range and LOD were reported to be 20 fM to 600 pM and 0.713 fM, respectively. This sensitive sensor had good applicability and reproducibility besides its facile acting mechanism.[136]

In another attempt, a bimetallic MOF probe was synthesized to detect miRNA-126, a glioma cancer biomarker. The CoNi-MOFs were stabilized on the gold electrode surface and later attached to the miRNA-126 complementary probes. The EIS response was altered in the presence of miRNA-126, creating a detection window for miRNA quantification. The sensor was linear from 1 fM to 10 nM and had an LOD of 0.14 fM. The main characteristics of this sensor field were easy to operate, rapid, sensitive, and reproducible.[137]

In a study done by Zhong *et al.*, Fe_3O_4@SiO_2@Au microspheres were synthesized and functionalized by hairpins (H1), which matched the target miRNA-522. Then, the Fe_3O_4@SiO_2@Au microspheres coated with H1 hairpins were magnetically separated and attached to the electrode's surface. In the presence of miRNA-522 and AuNPs/Zn MOFs (which were coated with H2 hairpins matched to H1), a catalyzed hairpin assembly process started, and electrochemiluminescence (ECL) signals were generated in parallel with miRNA-522 concentration. This study's LOD and linear range were 0.3 fM and 1 fM to 0.1 nM, respectively.[138]

The array of advantages associated with MOFs positions them as promising materials for biosensing platforms. Their merits, including rapid response times, cost-effectiveness, straightforward procedures, high loading capacity, potential for employing conjugated π-electron systems, porosity, and the presence of open metal sites, underscore their appeal. By offering tunable porosity and efficient probe immobilization,

Table 7 The novel metal material used in miRNA electrochemical sensors

miRNA	Nanoparticles and other electrode modifications	Electrochemical method	Linear range	Detection limit	Ref.
miR-21	MOF@Pt@MOF	DPV	1 fM–1 nM	0.29 fM	135
miR-21	Pd@MOF	DPV	20 fM–600 pM	0.713 fM	136
miR-126	CoNi-MOF	EIS	1 fM–10 nM	0.14 fM	137
miR-155	$Ti_3C_2T_x$ MXene nanosheets@FePcQDs	EIS	0.01 fM–10 pM	4.3 aM	144
miR-155	AuNPs/Ti_3C_2 MXene nanocomposite	DPV	1 fM–10 nM	0.35 fM	145
miR-122	AuHFGNs/P*n*BA–MXene	DPV	0.01 aM–10 nM	0.0035 aM	126
miR-21, miR-141	MXene–$Ti_3C_2T_x$ modified with AuNPs	EIS, CV	500 aM–50 nM	204 aM, 138 aM	146
miR-377	MXene–Au nanocomposites, AuNPs	SWV	10 aM–100 pM	1.35 aM	147

MOF: metal–organic framework, EIS: electrochemical impedance spectroscopy, DPV: differential pulse voltammetry, FePcQDs: iron phthalocyanine quantum dots, AuNPs: gold nanoparticles, AuHFGNs/P*n*BA: hierarchical flower-like gold, poly(*n*-butyl acrylate), SWV: square wave voltammetry.
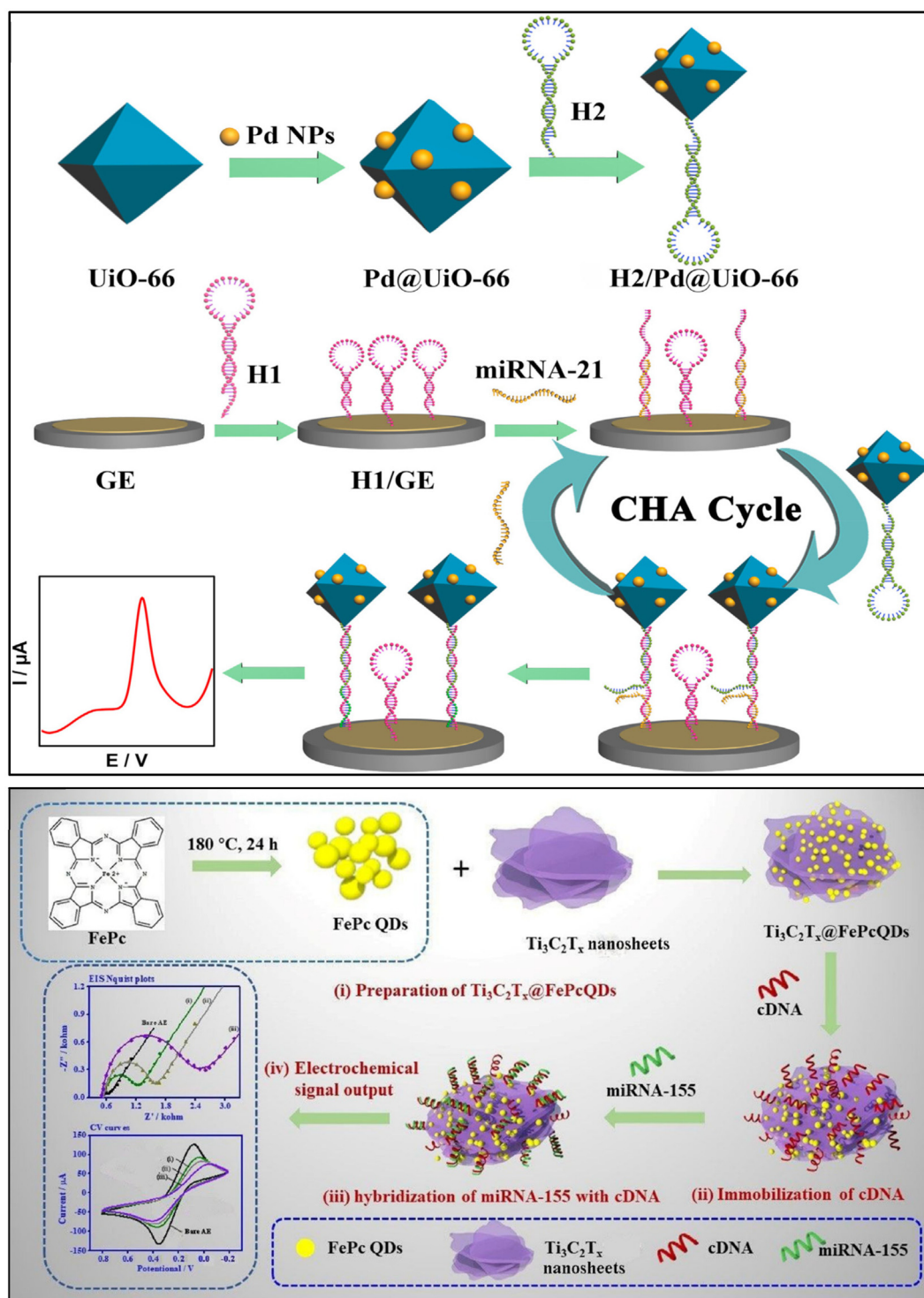
Fig. 10 (A) Electrochemical sensor based on the catalytic activity of Pd@MOF for miRNA-21 detection.[136] (B) miRNA-155 electrochemical sensor based on Ti$_3$C$_2$T$_x$ MXene nanosheets@FePcQDs structures.[144]

MOFs augment selectivity in biosensing applications. Nonetheless, it is imperative to note that MOFs are susceptible to environmental influences, necessitating meticulous handling to ensure sustained performance. Despite these considerable benefits, several critical challenges demand attention,

notably, instability in aqueous media, concerns regarding biological toxicity, and the need for a clearer understanding of their physiological effects.[137,139–141]

2.2.4.2. MXene. MXene was introduced in 2011 as a two-dimensional (2D) inorganic nanostructure with surface hydro-

philicity. They have a layered structure consisting of transition metals, carbon or nitrogen intervals, and various terminal groups. A general formula of $M_{n+1}X_nT_x$ represents all these differences in their structure. Their unique thermal, optical, and electronic features make them suitable for different biological and sensing applications.[142] Due to their electrocatalytic abilities, conductivity, and mechanical features, MXene has been considered to enhance the repeatability and stability of electrochemical sensors.[143] Duan et al. introduced an electrochemical nanobiosensor of miRNA-155. Iron phthalocyanine quantum dots (FePcQDs) were synthesized and decorated on the $Ti_3C_2T_x$ MXene nanosheets' surface. The $Ti_3C_2T_x$@FePcQDs nanostructures were attached to a gold electrode surface to enhance the efficiency. miRNA-155 complementary probes were attached to the $Ti_3C_2T_x$@FePcQDs nanostructure, affecting the impedance readings following the attachment to miRNA-155 (Fig. 10B). The dynamic response range and the LOD of the sensor were 0.01 fM–10 pM and 4.3 aM, respectively. This ultrasensitive sensor provided a facile and rapid real serum sample detection.[144]

Yang et al. developed another sensor for miRNA-155. In this sensor, AuNPs were decorated with Ti_3C_2 MXene to form AuNPs/Ti_3C_2 MXene nanocomposites, which were later immobilized on the GE. After that, the miRNA-155 complementary probes were attached to the composite with Au–S bonding. The 3′ end of the probe was tagged with MB molecules, generating electrochemical signals. In the presence of miRNA-155, a duplex formed between the miRNA and the complementary probe was subsequently cleaved by the exonuclease III (Exo III) after the MB release, and it was washed out. As a result, a decrease in the DPV signal, proportional to the concentration of miRNA, was noted. The reported linearity was 1 fM–10 nM, where the LOD was 0.35 fM. Stability, selectivity, and specificity are the main advantages of this sensor.[145]

In a study by Ranjbari et al., hierarchical flower-like gold, poly(n-butyl acrylate), and MXene (AuHFGNs/PnBA–MXene) nanocomposites were prepared on the electrode's surface, and antisense ssDNA complementary to miRNA-122 was immobilized on its surface. In the presence of the target miRNA and methylene blue electrochemical tag, the DPV signal increased. This sensor's LOD and linear range were reported to be 0.0035 aM and 0.01 aM to 10 nM, respectively. This sensor showed good stability, reproducibility, and specificity.[126]

Mohammadniaei et al. developed an electrochemical sensor for miRNA-21 and miRNA-141 detection. MXene–$Ti_3C_2T_x$ modified with AuNPs were captured on the screen-printed gold electrode. AuNPs were used to immobilize thiolated complementary DNA on the electrode's surface. Attaching this nanoparticle increased the electrochemical response 4 times with LOD of 204 aM and 138 aM for miRNA-21 and miRNA-141 detection, respectively.[146] Like the previous study, Wu et al. developed a biosensor based on the MXene–Au nanocomposites and AuNPs. MXene–Au nanocomposites were attached to the electrode's surface and immobilized with a complementary probe to the target miRNA. In the presence of the miRNA-377, another probe con-

taining AuNPs was attached to the other side of miRNA-377 bonded to the electrode's captured probes. In this way, the SWV signal enhanced 2.7-fold with a linear range from 10 aM to 100 pM. The sensor's LOD was 1.35 aM with good sensitivity, specificity, and selectivity in real human serum samples.[147]

Despite being in their infancy, MXenes are being extensively used due to various superior attributes, including but not limited to excellent electrical properties, large surface area, and acceptable biocompatibility.[148,149] However, achieving high stability, desirable sensitivity, and limited background signal are numerous challenges for upscaling these MXene-based nucleic acid biosensors. Hence, further research on more feasible synthesis methods and newer MXene nanocomposites to expand their use in this field is needed.[150,151] It can be concluded that MXene offers promise for various applications as a versatile nanomaterial with high conductivity and tunable surface chemistry.[148,152] Nonetheless, MXene synthesis can be complex, and more research is needed to fully understand its long-term stability and potential toxicity.[153]

2.3. DNA nanostructures and DNA nanomachines in miRNA biosensors

DNA nanostructures are promising nano-sized moieties with complex structures used in biosensors for signal amplification. They are programmable structures working based on the Watson–Crick base pairing and can interact with a large number of molecules such as proteins, viruses, and bacteria. They are widely used in sensors developed based on the complementary nature of two oligonucleotides or their replacement with a new DNA/RNA sequence with higher binding affinity.[154] Such electrochemical biosensors work by heating and annealing DNA hybrids to provide a sensitive and easy-to-make sensing platform.[155] Articles on DNA-nanostructure applications in miRNA detection are listed in Table 8.

DNA nanostructure-based biosensors are defined based on DNA nanostructures–analytes interactions, resulting in an altered structure in the DNA nano-conformation and thus a final measurable signal.[154] Three main categories and corresponding applications are illustrated in Fig. 11.

Lu et al. fabricated an ultrasensitive electrochemical biosensor using duplex-specific nuclease (DSN) and 3D DNA tetrahedron-structured probes (TSPs) for detecting serum miRNA-21. These probes comprised the target miR-21 and a hemin-labeled G-quadruplex sequence as a synergistic pseudo-enzyme for reducing H_2O_2 and oxidation of L-cysteine. The G-quadruplex/hemin acted as a horseradish peroxidase (HRP) alternative enzyme for electrocatalysis. The designed 3D DNA TSPs were immobilized on the Au electrode surface using Au–S bonding. With the target miR-21, the cleavage of DNA–RNA double strands by DSN will happen. Therefore, a major change in the reduction current was noted due to the release of miRNAs participating in the recycling step. The sensor was reported to have a broad linear range between 0.1 fM and 0.1 pM and an LOD of 0.04 fM. It could also directly measure miRNA-21 in real samples, providing reliable results. It was

Table 8 DNA nanostructures used in miRNA electrochemical sensors

miRNA	Nanoparticles and other electrode modifications	Electrochemical method	Linear range	Detection limit	Ref.
miR-155	DNA nanostructure	CV	50 fM to 1 fM	~0.5 fM	51
miR-21, miR-155, miR-196a, miR-210	DNA nanostructure	Amperometric	10 fM–1 nM, 10 fM–10 nM, 10 fM–10 nM, 10 fM–10 nM	10 fM	160
miR-01	DNA nanostructure	Amperometric	500 fM–10 nM	176 fM	159
miR-21	DNA nanostructure Au NPs	DPV	1.0 fM–10 nM	0.31 fM	161
miR-25	DNA nanostructure	DPV	1 fM–10 pM	0.3334 fM	157
miR-21	DNA nanostructure	DPV	0.1 fM–0.1 pM	0.04 fM	156
miR-21	DNA nanostructure	DPV	0.1 fM–1 nM	65 aM	162
miR-141	DNA nanostructure	CV	10 aM–10 pM	10 aM	67
miR-141	DNA nanostructure	CV	1 aM–10 nM	1 aM	89
miR-21	DNA nanostructure	SWV	10 fM–10 nM	3.6 fM	163
miR-196a	DNA nanostructure	DPV	0.05 fM–50 pM	15 aM	166
miR-21	DNA nanostructure	DPV	10^{-15} to 10^{-8} M	0.84 fM	168
miR-21, miR-155	Magnetic DNA nanospheres	SWV	5 fM–2 nM	1.5 fM and 1.8 fM	169
miR-21	DNA nanomachine, MOF	DPV	10 aM–10 pM	5.8 aM	170
miR-182-5p	DNA nanomachine	SWV	0.1 fM–1 nM	31.13 aM	171
miR-21	DNA nanomachine, AuNPs	SWV	100×10^{-18} to 100×10^{-12} M	39×10^{-18} M	172
miR-182	DNA nanomachine, AuNPs, and MB	DPV	1 fM–2 pM	0.058 fM	173
miR-21	DNA nanomachine, AuNPs, and NNPs	SWV	0.2 fM–1 nM	0.14 fM	174

DPV: differential pulse voltammetry, CV: cyclic voltammetry, AuNP: gold nanoparticle, AuAgNR: gold/silver nanorod, SWV: square wave voltammetry, MOF: metal–organic framework, MB: magnetic beads, MNPs: magnetic nanoparticles.

Fig. 11 Pie chart showing the distribution of DNA nanostructures in recent articles on miRNA biosensor.

concluded that the optimization of concentration and orientation of the probes using TSPs stable electrochemical signal production thanks to the synergistic effect of L-cysteine and G-quadruplex/hemin and using DSN for signal improvement was responsible for the high sensitivity and specificity of the miRNA biosensor.[156]

miRNA-25, a well-known biomarker for detecting heart failure and lung cancer, was the target of the nanobiosensor reported by Zhou *et al.* The authors used a competitive binding method using Y-shaped DNA (Y-DNA) nanostructures through non-linear hybridization chain reaction (non-linear hybridization chain reaction (HCR)) for miRNA-25 recognition. This research employed stable Y-shaped DNA nanostructures

and non-linear HCR as the capture probe and signal amplification, respectively. Y-DNA probes, consisting of a competitive probe (Y3) and supporting sequences (Y1, Y2), were immobilized on the Au electrode surface. After adding miRNA-25 as the target, the sequence was completely hybridized with Y3, and subsequently, the end triggers of Y1 and Y2 were blocked by Y3, initiating a non-linear HCR reaction. The biosensing platform revealed a broad linear range of 1 fM to 10 pM and an LOD of 0.3334 fM, with no need for enzymes or labels. This label-free miRNA biosensor showed remarkable selectivity by discriminating even single base mutations, which is ideal in clinical applications for the early and effective detection of different diseases.[157]

In another study, Tian *et al.* designed an electrochemical nanobiosensor using two signal-amplified strategies employing 3D nitrogen-doped rGO/AuNPs (3D N-doped rGO/AuNPs), a sensor platform and gold & silver nanorod/thionine/probe DNA (AuAgNR/Thi/F) as a detector element for miRNA-155 detection. To enhance the accessibility of the target biomolecule and lower the surface crowding effects, DNA tetrahedral nanostructures were fixed on the sensing electrode as the capture probes. The 3D N-doped rGO/AuNPs-modified electrode was fabricated *via* an electro-controlled co-reduction technique. After that, miR-155, along with AuAgNR/Thi/F composites, was placed on the electrode and detected using DPV measurements. Unlike the enzyme-based electrochemical biosensors, in which enzyme reduction occurs over time, metal NPs or redox mediators are highly stable labels. As reported, this nanobiosensor showed a dynamic range of 1×10^{-11} to 1×10^{-4} M and an LOD of 1×10^{-12} M with a proper performance in real sample analysis.[158]

Another miRNA biosensor used multi-branched DNA nanostructures composed of G-quadruplex wires and DNA concatamers. They were applied as the main part of the DNA nanoarchitectures fabricated using HCR. Hence, the G-quadruplex wires, used as branches, produced *via* the combination of the terminal deoxynucleotidyl transferase (TdT)-promoted polymerization and G-quadruplex parts. The DNA concatamers were straightly immobilized with the target miRNA on the Au working electrode. DNA concatamers had several biotin sites at the 5′-terminus, acting as a carrier to accumulate the biotinylated G-quadruplex wires *via* streptavidin/biotin interaction after adding streptavidin. After increasing the hemin level, the final signal was generated by forming G-quadruplex/hemin complexes in the DNA nanoarchitectures. The changes noted in the current were directly correlated to the miRNA-21 concentration. Using DPV measurement, a linear detection range and an LOD of 10 fM to 100 nM and 0.2 fM were recorded, respectively. The biosensor had high specificity to distinguish single-base mutations from the completely matched target miRNA-21. The sensor was reported to be capable of rapid, sensitive, and specific miRNA detection, showing a promising perspective in DNA-based clinical detection applications.[122]

Huang *et al.* fabricated an ultrasensitive miRNA biosensor using the famous tetrahedral DNA nanostructure with the amplification of the guanine nanowires. The DNA structure consisted of four single-strand oligonucleotides (A, B, C, and D) with a pendant hairpin capable of self-assembly. Tetrahedral B, C, and D were modified with thiol groups to help immobilize the DNA tetrahedral nanostructure on the Au electrode surface. Tetrahedral A was designed with a hairpin structure, which opened after the addition of target miRNA to the biosensing platform. With K^+ ion, a parallel G-quadruplex was formed by self-assembling the free stem section from the hairpin structure with a c-myc sequence at 3′ terminals. After adding c-myc sequences and Mg^{2+} ions, the parallel G-quadruplex stimulated the formation of a guanine nanowire. The amperometric measurements were based on the G-quadruplex/hemin complex formation and the H_2O_2/TMB redox reaction on the electrode surface. The miRNA nanobiosensor reached an LOD of 176 fM within a linear range of 500 fM–10 nM. Analyzing breast cancer serum samples, the proposed sensor demonstrated high selectivity, specificity stability, and practical utility.[159]

In another attempt, a sandwich-based electrochemical miRNA nanobiosensor was designed to simultaneously detect miR-21, miR-196a, miR-155, and miR-210 as key biomarkers for pancreatic carcinoma (PC). The capture probe in the form of DNA tetrahedral nanostructure was immobilized on a disposable electrode in the form of a 16-channel screen-printed gold electrode (SPGE). To optimize the hybridization step, two methods were compared. In the first approach, the hybridization solution, including different concentrations of target miRNAs and biotin-labeled signal probes, was immobilized on the DNA tetrahedron capture probe-modified SPGE surface. As for the second technique, various concentrations of target

miRNAs, followed by biotin-labeled signal probes, were added to the DNA tetrahedron capture probe/target miRNAs-16-channel SPGE. The enzymatic reaction helped with the recognition of the target miRNAs. Thus, the streptavidin-labeled poly-HRP40 was immobilized through biotin/avidin interaction. It was revealed that mixing the target miRNA with the signal probe before placing it on the electrode could improve the hybridization efficiency by overcoming the steric hindrance of these biomolecules. Hence, this strategy was used in further experiments due to its shorter incubation time. They used DNA tetrahedron nanostructures as a capture probe to reduce inter-strand interactions and enhance the hybridization efficiency. The final amperometric signal was generated due to the reduction of H_2O_2 when the TMB substrate was available. By taking advantage of the complementarity principle of the nucleic acid molecules, DNA tetrahedral nanostructure, and HRP enzyme activity, this electrochemical genosensor displayed an LOD of 10 fM along with a broad, seven times larger response range. The designed biosensing system was capable of the simultaneous and sensitive detection of the target miRNAs. In the proposed platform, the signal ratio increased due to the modifications applied to the electrode surface.[160]

Zhang *et al.* used a novel target recycling amplification and 2D DNA nanoprobe (DNP) methodology for constructing an electrochemical detection for precise miRNA-21 quantification. The GCE was modified with a gold crumbs (depAu) layer by the electrodeposition of $HAuCl_4$ aqueous solution. Then, the thiol-labeled capture probes (S1 and S2) were immobilized through the Au–SH bonds. Using hexanethiol (HT), the active sites of the electrode were blocked. A mixture of single-stranded A1 and the Fc-labeled strands of A2 and A3 was deposited to obtain the DNP structure. The Fc-labeled A2 and A3 sequences were hybridized with capture probes (S1 and S2), bringing the Fc-labels near the working electrode surface and, thus, a noticeable electrochemical signal. The mixture of annealed hairpin DNA (H) and miRNA-21 was deposited to recognize the target miRNA. The hairpin DNA was complementary to parts of the target sequence and single strand A1 in the DNP structure. After being hybridized with target miRNA-21, the prelocked toehold domain was opened. The hybridization of H and A1 based on the toehold-mediated strand displacement reactions (TSDRs) led to the detachment of the Fc-labeled A2 and A3 strands on the electrode surface and the release of miRNA-21, resulting in a dramatic decline in the output signal and target recycling process. The DPV sensor had an LOD of 0.31 fM and a linear concentration range of 1.0 fM to 10 nM. The excellent flexibility and stability of the bipedal DNP improved the immobilization process as well as the electrochemical signal response. Also, the DNP was efficiently regenerated through the one-step incubation of the three DNA strands and thus reduced the experiment cost significantly. Therefore, this nanobiosensor was suitable for sensitively assessing biomarkers.[161]

A hybrid structure composed of parallel structural dsDNA (PSD) and recombinant azurin (rAzu) was used for miRNA genosensor construction. The PSD was designed with Ag^+ ions

intercalating between mismatches (C–C) on top of each dsDNAs structure *via* covalent bonds. The rAzu metalloprotein acted as a selective spacer, providing a stable anchoring site for a single DNA strand at its N-terminus. The protein also acted as an electrochemical signal mediator to reduce Ag^+ ions. As the capture probe, the incomplete PSD was assembled on the rAzu-modified Au electrode. Then, different concentrations of target miR-155 were incubated on the rAzu/capture probe-modified electrode surface. There was an inverse relationship between the analyte concentration and current strength. As a result, decreasing the miRNA concentration from 50 fM to 1 fM significantly increased the silver ion (Ag^+) reduction current. Thanks to the high conductivity of the Ag-modified PSD and rAzu, an LOD of ~0.5 fM was obtained. The biosensor was reported to have similar results with quantitative real-time polymerase chain reaction (qRT-PCR). As for the qRT-PCR, however, the primer design is more complex, and the reverse transcription step may lead to experimental errors and extra costs. Therefore, the proposed biosensing system had a high capability for single mutation detection and miRNA expression profiling in cancer cells; it can, therefore, be used in developing different nanoscale biosensors and bioelectronic devices.[51]

An electrochemical sensor for exosomal miR-21 (exo-miRNA-21) detection was later developed by Liu *et al.* In this sensor, multiple DNA nanosheets (DNSs) were created using localized DNA cascade displacement reaction (L-DCDR), during which the target miRNA and complementary oligonucleotides were combined through the annealing process. Afterward, the MB molecules attached to the DNSs bond to the capture DNA on the electrode's surface *via* their free strands. Then, the amplified DPV signal for different miRNA concentrations was measured. This sensor was linear between the concentrations of 0.1 fM and 1 nM and had an LOD of 65 aM. Despite its great signal-to-noise ratio, high selectivity, and low LOD, the time-consuming annealing process (nearly 4 h) was a limiting factor in further applications.[162]

In another study, an electrochemical sensor was introduced for miRNA-141 as the prostate cancer biomarker. This platform formed a DNA tetrahedron structure probe (TSP) based on four designed oligonucleotides. An extended DNA then exited the tetrahedron structure and worked as the capture probe. TSPs were immobilized on the SPCE surface using the amine groups. With the target miRNA in the reaction, it was captured by the probes, changing the CV signals and providing a good detection opportunity with low background noise. The sensor was linear between 10 aM and 10 pM and had an LOD of 10 aM. Good stability and reproducibility were its other key features.[67]

In another attempt for miRNA-141, a two-step detection strategy was applied. In the first step, miRNA-141 bonds to a capture DNA in three parts: reporter (bond to biotinylated oligonucleotide), target (bind to the target miRNA), and adaptor region (bind to the framework nucleic acid (FNA) on the gold electrode). After that, the previous structure was exposed to FNA. In the presence of target miRNA, the first

nucleotide complex bonded to the FNA, and after that, the HRP-avidin complex was added. Afterward, the enzymatic HRP reaction generated recordable signals. The sensor had a linear response range between 1 aM and 10 nM and an LOD of 1 aM. The amplification-free process made sensing easier and more rapid, while the need for the enzymatic reaction increased the cost.[89]

Jiang *et al.* developed a sensitive sensor for miR-21. Three different hairpins were used in this platform: one specific for miR-21 and two assembled using the catalyzed hairpin assembly (CHA). One of its strands will attach to the linear double-stranded structure to form a DNA three-way junction (DNA TWJ), whereas the other one, which is complementary to the capture probes on the working electrode surface, attaches to MB. Therefore, the MB-oligo was released, attached to the electrode surface, and produced the SWV signals exposed to the target miRNA. The sensor had a linear range and LOD of 10 fM–10 nM and 3.6 fM, respectively. It could detect the target miRNA in real cancerous cells with good sensitivity and selectivity. However, the platform's complexity was the main limitation.[163]

A novel electrochemical sensor was introduced by Xu *et al.* for dual miRNA-21 detection and miRNA-155. A tetrahedron DNA nanostructure (TDN) was immobilized on the working gold electrode tailed by linking to a circular DNA capture probe. Target miRNA-21, miRNA-155, and two helper probes (each specific for one miRNA) bonded to the circular capture probe. Afterward, the Fc- and MB-probes were added and attached to miRNA-21 and miRNA-155, respectively. In this way, the electrochemical response of the Fc corresponded to miRNA-21, whereas that of MB depicted the miRNA-155 concentrations. The linear range was from 0.1 fM to 10 nM with an LOD of 18.9 aM and 39.6 aM for miRNA-21 and miRNA-155, respectively. Apart from being capable of multiplex detection of two miRNA in real cancerous cell lysate, being rapid, sensitive, and enzyme-free were the main advantages of this novel sensor.[164]

A new electrochemical sensor for exosomal miRNA-21 was developed by Miao *et al.* In this platform, the target miR-21 was hybridized using a template sequence and then polymerized to form a double-stranded molecule. This was followed by nick generation using a nicking enzyme (NEase), releasing a single-stranded sequence called TWJ2, and hybridization with its complementary probe known as TWJ1, which is attached to the gold electrode surface. Afterward, the dumbbell hybridization chain reaction (DHCR) using two dumbbell-shaped DNA structures occurred. The DHCR system provided a denser structure compared with the traditional hairpins. These dumbbell-shaped DNA structures were then converted into open flat-shaped structures, many attached to the electrode *via* TWJ1 and TWJ2 (Fig. 12A). The linear/dynamic range and LOD of the nanobiosensor were 10 aM to 100 fM and 7.3 aM, respectively. This platform generated a DNA nanostructure on the electrode surface for signal amplification, resulting in low and reliable LODs. The enzymatic reaction and RNA polymerization steps were, however, expensive and time-consuming. The sensor

Fig. 12 (A) Electrochemical detection of exosomal miRNA using strand displacement amplification[126] through dumbbell hybridization chain reaction (DHCR),[165] (B) three-dimensional magnetic DNA nanospheres for miRNA-21 and miRNA-155 detection.[169]

could detect miRNAs in both the cell lysate and serum samples.[165]

In a study by Guo *et al.*, a miRNA biosensor was developed using gold disk electrodes. The biosensor was based on a duplex-specific nuclease that triggers capture probe digestion from its 3′-PO$_4$ terminal, followed by the target recycling amplification. The capture probe's other end (3′-end) was then subjected to a nucleotide transferase reaction *via* terminal deoxy-

nucleotidyl transferase as a template-free DNA extension process. This resulted in the generation of ssDNA on the working electrode. The single-stranded nucleic acids absorbed the MB blue molecules, producing final signals. The miR-196a biosensor indicated ultra-sensitivity (15 aM) with a broad linear range (0.05 fM to 50 pM). It also had excessive specificity when tested against target miRNAs with a mismatched base. It was capable of successfully detecting miRNA-196a in plasma

samples of PC patients. The authors claimed their proposed biosensor to be simple, feasible, specific, and cost-effective; however, it was time-consuming as several in-step characterizations were needed.[166]

Recently, nanowires have attracted much attention in biosensor research. Wang and Hui used polyethylene glycol (PEG)–polypyrrole (PPy) nanowires to modify GCEs, which were then treated with a capture probe. The electrodes were then immersed in MB, followed by exposure to the target miRNA. The hybrid of target miRNA and capture probe resulted in a measurable reduction in the electrochemical signal due to the difference between the affinity of MB to ssDNA and dsDNA. Thanks to this competitive strategy, the biosensor showed an LOD of 0.033 pM and optimized capabilities. Compared with PPy nanowires-based biosensors, PEG/PPy nanowires had better electrical conductivity and antifouling properties for both single protein and complex human serum, suggesting its capability to be used for other types of DNA.[167]

With a novel approach and adapting self-assembled and continuous circular DNA, which was pH-sensitive, a team recently presented an electrochemical nanoswitch biosensor for miR-21. The authors described a complex of hexaammineruthenium(III) chloride ($[Ru(NH_3)_6]^{3+}$, RuHex) as a signal-generating agent that was electrostatically adsorbed on the negatively charged continuous annular DNA. When the target miRNA is available, RuHex generates a detectable electrochemical signal. Without target miRNA or unsuitable pH conditions, the nanoswitch was not activated. These phenomena were considered "signal on"/"signal off". The nanobiosensor could directly detect miRNA-21 in real samples (serum) with an LOD of 0.84 fM, without pretreatment.[168]

Shen et al. presented a novel sensor for detecting miRNA-21 and miRNA-155 as breast cancer biomarkers. The Fe_3O_4 nanospheres were coated with AuNPs, and subsequently, a core magnetic nanosphere coated with a DNA-branched structure was fabricated through a hyperbranched hybridization chain reaction (HHCR). Later, these particles were bonded to gold stirbars via complementary DNA hybridization. Target miRNAs could be replaced with the magnetic DNA nanospheres, containing two electrochemical probes in their branched oligonucleotides, Fc and MB, each corresponding to a target miRNA. The magnetic DNA nanospheres were released after adding miRNA and captured on the electrode through the magnetic field. The SWV curves corresponding to the Fc and MB molecules were recorded (Fig. 12B). The enzyme-free and sensitive platform had a linear range between 5 fM and 2 nM and an LOD of 1.5 fM and 1.8 fM for miRNA-21 and miRNA-155, respectively.[169]

DNA nanomachines are molecular moving structures responsible for signal amplification. In a study by Bao et al., polydopamine nanoparticles (PDANs) were functionalized with miRNA-21 complementary hairpins (HP1) and hairpins (HP2). Following the attachment of HP1 and miRNA-21, HP2 was added. Then, miRNA-21 was recycled to trigger more hairpin assembly. After that, a machine-like structure attached to the hairpins on the electrode surface (HP3) was formed.

Exonuclease-3 enzyme was used to cut the walking legs of the PDANs (complementary sequence between HP2 and HP3). Walking continued until all HP3 was cut and stranded. Then, the two other hairpins (A1 and A2) were added to the system to form a dendrimer-like structure by forming a hybridization assembly between A1, A2, and the stranded probe on the electrode. The MOF probes ($Fe-MIL-88-NH_2$ MOF bonded to the HP4) were then assembled with the dendrimer-like structure, and an electrochemical probe (Prussian blue) was generated on the porous MOF structure. Prussian Blue (PB) amplified the signal, recorded through the DPV electrochemical measurement. The measured linearity and LOD were 10 aM to 10 pM and 5.8 aM, respectively. The novel sensor was user-friendly, sensitive, and worked in ambient conditions.[170]

An electrochemical nanobiosensor of miR-182-5p was introduced by Chang et al., a DNA structure in the form of a three-way junction (TWJ) by annealing a specific linear sequence. In the presence of miRNA-182-5p, an annular DNA walker was formed and attached to TWJ. The layer had three recognition sites for the hairpin-bind Fc immobilized on the GCE surface. When the two sites met each other, the Nt.BstNB I endonuclease cleaved the double strand created between the TWJ recognition sites and fixed the hairpins. Following this process, Fc molecules were released and washed out, while TWJ, as an annular walking machine, continued cleaving more hairpin-Fc structures. The robust SWV electrochemical signal caused by Fc molecules significantly decreased in the presence of target miRNA when TWJ started the hairpin cleavage. This innovative sensor was rapid and sensitive but not cost-effective because of the enzymatic reactions. The reported linear range was from 0.1 fM to 1 nM, and the LOD was 31.13 aM.[171] Miao et al. developed a promising electrochemical sensor for miRNA-21 detection. In their research, probe a was immobilized on the surface of the AuNPs and gold electrodes. Probe b, on the other hand, was assembled with probe a through its 3′ end region, forming a triplex DNA structure. With the availability of the target miRNA, which is complementary to probe b, a duplex-specific nuclease (DSN) happened to utilize Nb.BbvCI NEase. This phenomenon helps release miRNA-21 to promote recycling by attaching to the neighboring probe b on the AuNPs surface.

On the other hand, probe c is assembled with probe a, immobilized on the gold electrode through its 3′ end. The 5′ end of probe c was attached to the MB molecules, enhancing the electrochemical response by helping with tris(2-carboxyethyl)phosphine hydrochloride (TCEP). In the presence of the target miRNA-21, the SWV signal was measured. In its absence, on the other hand, the complete sequence of probe b assembled with probe c, generating a duplex cut by NEase. After that, the MB molecules were detached, and the electrochemical response was decreased. AuNPs walked on the surface of the working electrode with probe b–probe c duplexes amplifying the signals. The dynamic range and LOD of the current were 100×10^{-18} to 100×10^{-12} M and 39×10^{-18} M, respectively. The attachment and detachment process of the three probes was: probe a, a thiolated probe,

covalently bonded to the AuNPs and Au-electrode; probe b and probe c assembled with probe a based on the pH condition. In acidic pH, these probes were attached, while they were detached in alkaline pH. This phenomenon caused a controllable attachment and detachment of the two probes, simplifying probe reconstruction in the sensor. This novel sensor was rapid, sensitive, selective, and suitable for POC applications (Fig. 13A).[172]

In another sensor for miRNA-182, AuNPs were attached to the magnetic beads. A DNA-walker and Fc-probe were stabilized on the AuNP surface subsequently. The free end of the DNA-walker was duplexed with a probe that could attach to the target miRNA, and the free end bonded to the Fc-probe through the strand displacement reaction (SDR). The addition of NEase resulted in a duplex between the walker and the Fc-probe being cut by the nicking enzyme, releasing the Fc mole-
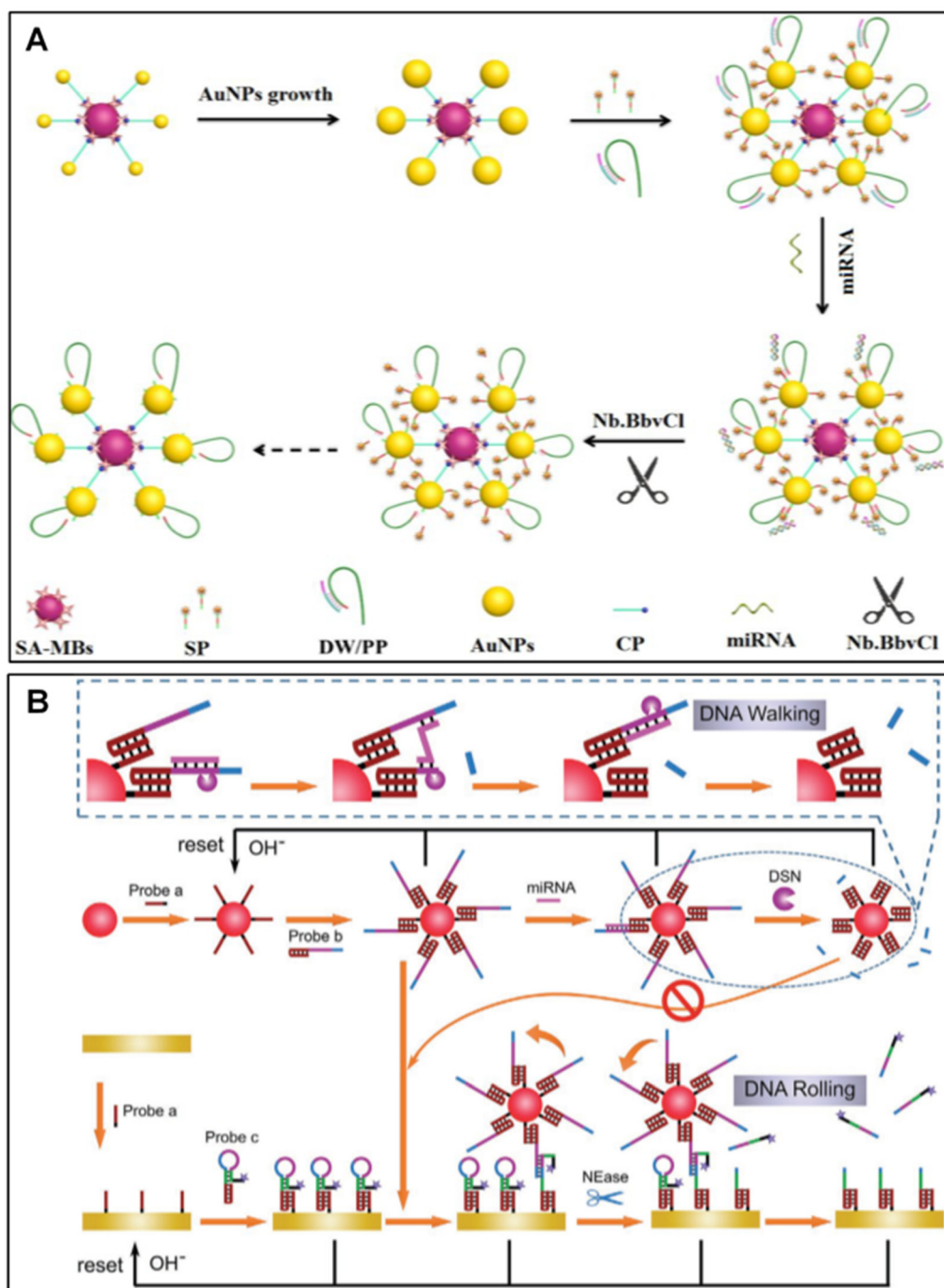
Fig. 13 DNA-machine electrochemical sensors (A) working with four different probes, AuNPs, and duplex-specific nuclease activity for miRNA-21 detection.[172] (B) AuNPs attached to the magnetic beads formed a DNA-walker machine for miRNA-182 detection.[173]

cules and washing out from the electrode. As a result, a decrease was noted in the electrochemical signal (Fig. 13B). The sensor had good selectivity and sensitivity in real serum samples. It was linear from 1 fM to 2 pM and had an LOD of 0.058 fM.[173]

Zhang *et al.* fabricated an electrochemical sensor for miRNA-21 detection. AuNPs were immobilized using oligonucleotides bonded to the hairpin (HP1) functionalized with an MB electrochemical probe. The magnetic nanoparticles (MNPs) were immobilized using the second hairpin (HP2). In the presence of the target miRNA, they assembled with HP1 and were completely detached from the AuNPs. Afterward, during strand hybridization, HP1 was attached to HP2 on the surface of the MNPs, releasing and recycling miRNA-21 to generate higher signals. After that, MNPs were magnetically captured on the electrode surface, where SWV signals were recorded based on the MB molecules attached to the MNPs on HP1. The sensor detected miRNA-21 in 25 minutes with an LOD of 0.14 fM. The platform was linear between 0.2 fM and 1 nM. High sensitivity and good reaction speed were the most important features of the sensor.[174]

Based on our discussion here in this section, it can be concluded that DNA nanotechnology has made substantial contributions to biosensing technology, primarily due to its attributes such as rigidity, water-solubility, biodegradability, and biocompatibility. DNA-based sensors excel in achieving high selectivity and specificity through molecular recognition and amplification processes.[175,176] Nevertheless, it is essential to acknowledge that these promising structures come with challenges that limit their practical application, particularly in biosensing. The design and assembly of DNA-based nanostructures can be intricate, and their performance may exhibit sensitivity to environmental conditions, which can impact their reliability. One of the most pressing concerns lies in the instability of DNA nanostructures when subjected to real sample analysis. The dilution of these structures in biological fluids can alter their assembly and functionality, posing a significant obstacle to their use.[177,178] Additionally, the proposed strategies for stabilizing these materials often introduce additional sample pretreatment steps or complicate the design, which may need to be more conducive to biosensor fabrication. Moreover, using DNA nanostructures in miRNA biosensors elevates the risk of encountering false positive responses or background signals due to unspecific interactions between these structures and non-target nucleic acids.[54,179]

3. Comparative analytical performance of nanomaterials in miRNA biosensors

3.1. Enhanced sensitivity

Nanomaterials, such as the graphene family (including graphene, GO, and rGO),[180–182] CNTs,[183] CNFs,[184] AuNPs,[97] and AgNPs,[185] significantly boost the sensitivity of miRNA biosensors. Graphene-based materials stand out for their exceptional electrical conductivity, large surface area, and ease of functionalization, all contributing to heightened sensitivity.[180–182] Similarly, CNTs and CNFs, known for their high aspect ratio and exceptional electrical properties, enable efficient miRNA probe immobilization, resulting in highly sensitive measurements.[183,186] AuNPs, with enhanced conductivity and easy functionalization, offer improved sensitivity and selectivity.[97,110] AgNPs, with catalytic activity and large surface areas, amplify signals and enhance sensitivity.[187] These nanomaterials are selected for miRNA biosensors based on specific application needs to achieve superior sensitivity in miRNA biosensors.

3.2. Selectivity and specificity

Regarding selectivity and specificity, the graphene family stands out due to its easy functionalization, enabling tailored miRNA capture probe design and specific binding with target miRNAs.[181] Moreover, the versatile surface functionalities of graphene materials contribute to reduced non-specific interactions, enhancing the overall selectivity.[181,188] Similarly, AuNPs and their composites significantly improve selectivity and specificity.[97] Their easy functionalization simplifies the attachment of miRNA capture probes, ensuring selective immobilization. Furthermore, specific functionalization and control over probe design enhance the selectivity of biosensors, reducing false positives.[110,189]

Meanwhile, AgNPs and their composites enhance specificity through catalytic activity, leading to specific reactions and improved sensor selectivity. Precise control over probe immobilization on AgNPs ensures specific binding with target miRNAs, reducing false positives.[190] Metal–organic frameworks (MOFs) offer tunable porosity, enabling selective miRNA capture and immobilization, while the encapsulation of guest molecules in MOFs further enhances biosensor specificity.[124,191] DNA-based sensors, such as DNA nanostructures and nanomachines, excel in molecular recognition and amplification, ensuring precise and specific binding with target miRNAs. These sensors reduce non-specific interactions through their tailored design, leading to high selectivity and specificity, particularly in complex matrices.[54]

3.3. Application flexibility

For application flexibility, almost all carbon-based materials offer biocompatibility and low cytotoxicity, making them suitable for biological applications. Researchers can choose these materials based on specific requirements, such as optical properties or biocompatibility, allowing them to adapt to diverse settings.[93,186,192] Magnetic nanoparticles, including iron oxide nanoparticles, enable easy separation and concentration of target miRNAs, a valuable feature, especially in complex sample matrices.[130] Some metal nanoparticles, such as platinum and palladium, are also selected for their catalytic properties in specific sensing strategies, expanding their application versatility.[193,194] The emerging nanomaterial MXene, offers high electrical conductivity for improved electron trans-

Table 9 Comparative analysis of nanomaterials used in electrochemical miRNA sensors

Nanomaterials		Main impacts on performance
Carbon-based nanomaterials in miRNA biosensor	Graphene family	• Enhanced conductivity • High surface area • Selectivity • Sensitivity
	Nanotubes and nanofibers	• Enhanced aspect ratio • Mechanical strength • Rapid electron transfer • Sensitivity
	Other carbon-based	• Easy functionalization • Biocompatibility
Metal nanoparticles in miRNA biosensors	AuNPs and composites	• Enhanced conductivity • Easy functionalization • Signal amplification • Sensitivity
	Silver nanoparticles and composites	• Catalytic activity • Signal amplification • Selective immobilization
	Magnetic and other metal nanoparticles	• Magnetic manipulation • Enhanced catalytic properties
	Metal–Organic Framework (MOF)	• Tunable porosity • Application flexibility • Sensitivity
	MXene	• High conductivity • Tunable surface chemistry • Sensitivity
DNA nanostructures and DNA nanomachines		• Molecular recognition • Application in complex matrices

fer kinetics in various sensing strategies. Its tunable surface chemistry allows for tailored functionalization, making it suitable for various applications.[148,195] DNA-based sensors demonstrate their effectiveness across diverse applications, maintaining their robust performance even in complex biological matrices.[54] The combination of molecular recognition and amplification ensures that they are well-suited for various clinical and environmental applications, showcasing their adaptability to different settings (Table 9).[196]

4. Conclusion and future perspectives

To date, miRNAs have been accepted as a remarkable diagnostic marker for the early detection of various diseases, including cancers. The introduction of various biosensors has been an important reason behind this as they have helped overcome the challenges of quantifying and monitoring these small molecules with high homologous sequences. As mentioned in this article, the use of different nanomaterials in electrochemical platforms has offered additional analytical features, including higher specificity, feasible portability, and flexible design capability coupled with fast and accessible analysis technologies. It was concluded that the future of miRNA detection using nanomaterials relies on methods to control the immobilized strands as well as the electrode itself. This is because using a combination of different nanomaterials such as nano-ribbons, -tubes, -particles, and -sheets for electrode treatment or miRNA detection helped improve the LoD of such systems. Therefore, they offer promising platforms for clinics to measure various miRNAs, enabling the early diagnosis of many diseases.

Despite significant advancements in the field, the commercialization of miRNA nanobiosensors encounters substantial hurdles. These challenges encompass the high complexity of fabricating multilayered devices incorporating biomolecules, which presents difficulties in reproducibility. Furthermore, concerns regarding biocompatibility arise due to the use of nanomaterials, raising questions about biosafety, biocompatibility, and environmental considerations. The cost issue remains an obstacle as the promise of reduced pricing through miniaturization may not render these screening and diagnostic processes cost-effective. Achieving a desirable shelf-life while maintaining sensitivity and specificity poses an additional challenge for miRNA point-of-care devices. Beyond fabrication challenges, a majority of reported miRNA nanobiosensors need more evaluation and validation using real samples, necessitating further studies to address these practical assessment challenges. Despite decades of research on miRNA sensors, they have not been commercialized due to stability and shelf-life issues. However, novel electrodes and modification methods can improve electrochemical sensor durability and robustness, making miRNA sensors more stable and long lasting. Switching from large and immobile equipment to smaller and more portable versions would speed up commercialization and allow for innovative electrode 3D printing. Current miRNA detection methods are complicated and expensive; thus, future studies should focus on simplifying and streamlining methodologies to improve the accessibility and cost-effectiveness. This involves developing affordable and accessible diagnostic tools to identify miRNA in various clinical settings, making this technology more accessible to everyone.

The future of miRNA nanobiosensors is connected to three main improvements: simultaneous detection of multiple miRNAs, wearable and portable nanobiosensors, and simplicity of designs toward commercialization. The simultaneous detection of several miRNAs is crucial to ensure diagnostic accuracy and identify multiple diseases simultaneously. It is essential to have multiplex detection methods that can identify several miRNAs in one test for miRNA analysis. This technology would enable faster detection of many diseases and improve sickness screening, helping to understand an individual's health. High sensitivity is required for miRNA detection, and novel nanomaterials and nanocomposites are necessary to improve miRNA

sensor sensitivity, allowing them to detect miRNAs at lower concentrations. Novel amplification methods will increase sensitivity, allowing the detection of even small amounts of miRNAs. Wearable and portable biosensors are essential for miRNA detection progress. These gadgets will allow real-time miRNA profiling, enabling continuous health monitoring. Mobile apps will enable people to get feedback and notifications quickly for illness management and prevention. Future studies should focus on new sample sources like tears and sweat to make miRNA detection more convenient and less invasive. These body fluids can retrieve miRNAs without pain or invasiveness, making miRNA expression pattern analysis efficient and stress-free, especially when blood-based methods are inadequate or problematic. Developing efficient methods for collecting and analyzing alternative sample sources is crucial to ensuring efficiency, which will be studied in future research. The development of portable and point-of-care devices for the rapid on-site analysis of microRNAs in clinical settings has been significantly impacted by miniaturization enabled by nanomaterials. Furthermore, integrating nanomaterials with microfluidic technology allows for the creation of miniaturized and cost-effective testing devices, reducing the need for complex laboratory infrastructure. However, using nanomaterials in diagnostic devices may raise concerns about their potential toxicity and long-term effects on human health.

Abbreviations

NPs	Nanoparticles
LOD	Limit of detection
WO_3	Tungsten trioxide
Au–Pt nanoparticles	Gold–platinum nanoparticles
SPCE	Screen-printed carbon electrode
rGO	Reduced graphene oxide
PCA	Pyrene carboxylic acid
AuNPs	Gold nanoparticles
Fc-SH	6-Ferrocenylhexanethio
AgNPs	Silver nanoparticles
CNT	Carbon nanotube
GQDs	Graphene quantum dots
GO	Graphene oxide
AQ	Anthraquinone
MB	Methylene blue
PDA	Polydopamine
SWV	Square wave voltammetry
ZrO_2	Zirconium dioxide
GNR	Gold nano-rods
DPV	Differential pulse voltammetry
MCH	6-Mercaptohexanol
SA-ALP	Streptavidin-conjugated alkaline phosphates
AAP	2-Phosphate
AA	Ascorbic acid
H-bonds	Hydrogen bonds
PPY/MWCNTs/PB	Multiwalled carbon nanotubes/Prussian blue-functionalized polypyrrole nanowire array
SWCNTs	Single-walled carbon nanotubes
Thi	Thionin
S-MWCNTs	Shortened multiwalled carbon nanotubes
A-MWCNTs	Acidified multiwalled carbon nanotubes
CNNS	Carbon nitride nanosheets
DSN	Duplex-specific nuclease
Ag@Au core–shell/ GQDs	Silver–gold core–shell nanoparticles conjugated with graphene quantum dots
PNA	Peptide nucleic acid
LOQ	Limit of quantification
FC60	Fullerene nanoparticles
HRP	Horseradish peroxidase
LIG	Laser induced graphene
PI	Polyimide
$[Fe(CN)_6]^{3-/4-}$	Potassium ferro/ferricyanide
Fc	Ferrocene
EATR	Enzyme-assisted target recycling
EIS	Electrochemical impedance spectroscopy
SPR	Surface plasmon resonance
MMBs	Magnetic microbeads
AuNP-MMBs	AuNP-coated MMBs
ODN	Oligonucleotide
MoS_2	Molybdenum disulfide
$AuNPs/MoS_2$	AuNPs/hollow MoS_2 microcubes
EEC	Electrochemical–chemical–chemical
SAuNWE	Single Au nanowire electrode
MB-CP	Hairpin capture probes harboring methylene blue tags
Fc-CPs	Ferrocene labeled aptamer probes
CEAM	Cyclic enzymatic amplification method
AuNPs@Dox	Doxorubicin-loaded gold nanoparticles
DHP	Double-loop hairpin probe
TdT	Terminal deoxynucleotidyl transferase
3D	Three-dimensional
sDNAs	Signal DNAs
SAM	Self-assembled monolayer
JUG-SH	5-Hydroxy-3-hexanedithiol-1,4-naphthoquinone
6-MHA	6-Mercaptohexanoic acid
AuNPs/GCE	AuNPs-modified glassy carbon electrode
Pd@HRP	Porous palladium-modified HRP sphere
S/N	Signal to noise
GNF@Pt	Gold nanoflower/platinum electrode
MB/barG	Barcode-gold nanoparticles
Au-PWE	Au-paper working electrode
MOF	Metal organic framework
SLNPs	Single-layer MoS_2-AuNPs
MLNPs	Multilayer MoS_2-AuNPs
FTO	Fluorine-doped tin oxide electrode
MU	11-Mercapto-1-undecanol
CP	Capture probe
SP	Stacking probe
AuNP–PNT	Peptide nanotubes-decorated gold nanoparticles
PPY	Polypyrrole
GP	Graphene

CVs	Cyclic voltammograms
GCE	Glassy carbon electrode
SAM	Self-assembled monolayer
CuMOFs	Modified Cu-based metal–organic frameworks
PNT	Peptide nanotubes
Pt	Platinum
Ag	Silver
AFP	Alpha fetoprotein
HCC	Hepatocellular carcinoma
ConA	Concanavalin A
POC	Point-of-care
AgNW	Silver nanowire
MPBA	4-Mercaptophenylboronic acid
LSV	Linear-sweep voltammetry
GCE	Glassy carbon electrode
GA	Glutaraldehyde
AgNF	Silver nanofoam
PEI–AgNPs	Polyethene imine silver nanoparticles
AuNW	Gold nanowire
AuAgNR	Gold and silver nanorod
TMB	3,3′,5,5′-Tetramethylbenzidine
TCEP	Electrochemical active molecule
NRs	Nanorods
pd-MoS$_2$ NSs	Polyoxometalate-derived MoS$_2$ nanosheets
cDNA	Complementary DNA
MGCE	Magnetic glassy carbon electrode
CHA	Catalytic hairpin assembly
SEECBS	Single-entity electrochemistry biosensing
MNPs	Magnetic nanoparticles
ssDNA	Single strand DNA
LNA	Locked nucleic acid
RCA	Rolling circle amplification
SDA	Strand displacement amplification
PBIB	Propargyl-2-bromoisobutyrate
eATRP	Electrochemically-mediated atom transfer radical polymerization
FMMA	Ferrocenylmethyl methacrylate
NiPN	Nickel phosphate nanostructure
MBCPE	Carbon paste electrode containing magnetic bar
RSV	Resveratrol
dsDNA	Double strand DNA
MGCE	Magnetic glassy carbon electrode
PtNPs	Platinum nanoparticles
AuNF	Gold nanoflower
GE	Gold electrode
PER	Primer exchange reaction
AP	Paracetamol
2D	Two-dimensional
FePcQDs	Iron phthalocyanine quantum dots
Exo III	Exonuclease III
TSPs	Tetrahedron-structured probes
Y-DNA	Y-shaped DNA

non-linear HCR	Non-linear hybridization chain reaction
3D N-doped rGO/AuNPs	3D nitrogen-doped reduced graphene oxide/gold nanoparticles
AuAgNR/Thi/F	Gold and silver nanorod/thionine/complementary DNA
HCR	Hybridization chain reaction
Gus	G-quadruplex units
TMB	Tetramethyl benzidine dihydrochloride
PC	Pancreatic carcinoma
SPGE	Screen-printed gold electrode
DNP	DNA nanoprobe
depAu	Gold particles
HT	Hexanethiol
TSDRs	Toehold-mediated strand displacement reactions
PSD	Parallel structural dsDNA
rAzu	Recombinant azurin
qRT-PCR	Quantitative real-time polymerase chain reaction
exo-	Exosomal
DNSs	DNA nanosheets
L-DCDR	Localized DNA cascade displacement reaction
TSP	Tetrahedron structure probe
FNA	Framework nucleic acid
TWJ	Three-way junction
TDN	Tetrahedron DNA nanostructure
NEase	Nicking enzyme
DHCR	Dumbbell hybridization chain reaction
HHCR	Hyperbranched hybridization chain reaction
PDANs	Polydopamine nanoparticles
HP/H	Hairpin
PB	Prussian blue
TCEP	Tris(2-carboxyethyl)phosphine hydrochloride
SDR	Strand displacement reaction
MB	Magnetic beads
PEG	Polyethylene glycol
$[Ru(NH_3)_6]^{3+}$, RuHex	Hexaammineruthenium(III) chloride
GC	Gastric cancer
CRISPR	Clustered regularly interspaced short palindromic repeats
PMO	Phosphorodiamidate morpholino oligos

Conflicts of interest

There are no conflicts to declare.

References

1 A. A. Jamali, *et al.*, Nanomaterials on the road to microRNA detection with optical and electrochemical

nanobiosensors, *TrAC, Trends Anal. Chem.*, 2014, **55**, 24–42.

2 Z. Shabaninejad, *et al.*, Electrochemical-based biosensors for microRNA detection: Nanotechnology comes into view, *Anal. Biochem.*, 2019, **581**, 113349.

3 A. Lujambio and S. W. Lowe, The microcosmos of cancer, *Nature*, 2012, **482**(7385), 347–355.

4 T. Kilic, *et al.*, microRNA biosensors: opportunities and challenges among conventional and commercially available techniques, *Biosens. Bioelectron.*, 2018, **99**, 525–546.

5 T. Tian, J. Wang and X. Zhou, A review: microRNA detection methods, *Org. Biomol. Chem.*, 2015, **13**(8), 2226–2238.

6 L. Xu, *et al.*, Optical, electrochemical and electrical (nano) biosensors for detection of exosomes: A comprehensive overview, *Biosens. Bioelectron.*, 2020, **161**, 112222.

7 C. Karunakaran, R. Rajkumar and K. Bhargava, Introduction to Biosensors, in *Biosensors and Bioelectronics*, ed. C. Karunakaran, K. Bhargava and R. Benjamin, Elsevier, 2015, ch. 1, pp. 1–68.

8 Y. Huang, *et al.*, Disease-Related Detection with Electrochemical Biosensors: A Review, *Sensors*, 2017, **17**(10), 2375.

9 P. Malik, *et al.*, Emerging nanomaterials for improved biosensing, *Meas.: Sens.*, 2021, **16**, 100050.

10 X. Huang, Y. Zhu and E. Kianfar, Nano Biosensors: Properties, applications and electrochemical techniques, *J. Mater. Res. Technol.*, 2021, **12**, 1649–1672.

11 H. Wang, *et al.*, Selective Single Molecule Nanopore Sensing of microRNA Using PNA Functionalized Magnetic Core–Shell Fe_3O_4–Au Nanoparticles, *Anal. Chem.*, 2019, **91**(12), 7965–7970.

12 T. Liao, *et al.*, Ultrasensitive Detection of MicroRNAs with Morpholino-Functionalized Nanochannel Biosensor, *Anal. Chem.*, 2017, **89**(10), 5511–5518.

13 Z. Jiang, *et al.*, Novel electrochemical biosensing platform for microRNA: bivalent recognition-induced nanoparticle amplification occurred in nanochannels, *Sens. Actuators, B*, 2021, 130209.

14 A. De La Escosura-Muñiz and A. Merkoçi, Nanochannels preparation and application in biosensing, *ACS Nano*, 2012, **6**(9), 7556–7583.

15 B. Lenhart, *et al.*, Nanopore fabrication and application as biosensors in neurodegenerative diseases, *Crit. Rev. Biomed. Eng.*, 2020, **48**(1), 29–62.

16 M. Rahman, *et al.*, Recent advances in integrated solid-state nanopore sensors, *Lab Chip*, 2021, **16**, 3030–3052.

17 Z. Jiang, *et al.*, Novel electrochemical biosensing platform for microRNA: Bivalent recognition-induced nanoparticle amplification occurred in nanochannels, *Sens. Actuators, B*, 2021, **344**, 130209.

18 C. E. Angevine, *et al.*, Laser-based temperature control to study the roles of entropy and enthalpy in polymer-nanopore interactions, *Sci. Adv.*, 2021, 7(17), eabf5462.

19 A. Nehra, S. Ahlawat and K. P. Singh, A biosensing expedition of nanopore: a review, *Sens. Actuators, B*, 2019, **284**, 595–622.

20 H.-L. Shuai, *et al.*, Au nanoparticles/hollow molybdenum disulfide microcubes based biosensor for microRNA-21 detection coupled with duplex-specific nuclease and enzyme signal amplification, *Biosens. Bioelectron.*, 2017, **89**, 989–997.

21 F. Sicard, *et al.*, Targeting miR-21 for the therapy of pancreatic cancer, *Mol. Ther.*, 2013, **21**(5), 986–994.

22 S. R. Pfeffer, C. H. Yang and L. M. Pfeffer, The role of miR-21 in cancer, *Drug Dev. Res.*, 2015, **76**(6), 270–277.

23 X. Pan, Z.-X. Wang and R. Wang, MicroRNA-21: a novel therapeutic target in human cancer, *Cancer Biol. Ther.*, 2010, **10**(12), 1224–1232.

24 G. Mahesh and R. Biswas, MicroRNA-155: a master regulator of inflammation, *J. Interferon Cytokine Res.*, 2019, **39**(6), 321–330.

25 N. Suzuki, *et al.*, Chiral graphene quantum dots, *ACS Nano*, 2016, **10**(2), 1744–1755.

26 F. R. Simões and M. G. Xavier, Electrochemical sensors, *Nanoscience and its Applications*, 2017, pp. 155–178.

27 R. Sivaranjanee, *et al.*, Electrochemical sensing system for the analysis of emerging contaminants in aquatic environment: A review, *Chemosphere*, 2022, 133779.

28 K. D. Patel, R. K. Singh and H.-W. Kim, Carbon-based nanomaterials as an emerging platform for theranostics, *Mater. Horiz.*, 2019, **6**(3), 434–469.

29 J. Peña-Bahamonde, *et al.*, Recent advances in graphene-based biosensor technology with applications in life sciences, *J. Nanobiotechnol.*, 2018, **16**(1), 1–17.

30 H. Jiang, *et al.*, Miniaturized paper-supported 3D cell-based electrochemical sensor for bacterial lipopolysaccharide detection, *ACS Sens.*, 2020, **5**(5), 1325–1335.

31 J. Bao, *et al.*, An enzyme-free sensitive electrochemical microRNA-16 biosensor by applying a multiple signal amplification strategy based on Au/PPy-rGO nanocomposite as a substrate, *Talanta*, 2019, **196**, 329–336.

32 A. Ebrahimi, *et al.*, Design, development and evaluation of microRNA-199a-5p detecting electrochemical nanobiosensor with diagnostic application in Triple Negative Breast Cancer, *Talanta*, 2018, **189**, 592–598.

33 D. Isin, E. Eksin and A. Erdem, Graphene oxide modified single-use electrodes and their application for voltammetric miRNA analysis, *Mater. Sci. Eng., C*, 2017, **75**, 1242–1249.

34 C. Ingrosso, *et al.*, Au nanoparticle in situ decorated RGO nanocomposites for highly sensitive electrochemical genosensors, *J. Mater. Chem. B*, 2019, **7**(5), 768–777.

35 R. Salahandish, *et al.*, Label-free ultrasensitive detection of breast cancer miRNA-21 biomarker employing electrochemical nano-genosensor based on sandwiched AgNPs in PANI and N-doped graphene, *Biosens. Bioelectron.*, 2018, **120**, 129–136.

36 A. Bharti, N. Agnihotri and N. Prabhakar, A voltammetric hybridization assay for microRNA-21 using carboxylated graphene oxide decorated with gold-platinum bimetallic nanoparticles, *Microchim. Acta*, 2019, **186**(3), 185.

37 H.-L. Shuai, *et al.*, Ultrasensitive electrochemical sensing platform for microRNA based on tungsten oxide-graphene

composites coupling with catalyzed hairpin assembly target recycling and enzyme signal amplification, *Biosens. Bioelectron.*, 2016, **86**, 337–345.

38 M. Azimzadeh, *et al.*, Early detection of Alzheimer's disease using a biosensor based on electrochemically-reduced graphene oxide and gold nanowires for the quantification of serum microRNA-137, *RSC Adv.*, 2017, **7**(88), 55709–55719.

39 M. Zouari, *et al.*, Determination of miRNAs in serum of cancer patients with a label-and enzyme-free voltammetric biosensor in a single 30-min step, *Microchim. Acta*, 2020, **187**(8), 1–11.

40 M. Zouari, *et al.*, Femtomolar direct voltammetric determination of circulating miRNAs in sera of cancer patients using an enzymeless biosensor, *Anal. Chim. Acta*, 2020, **1104**, 188–198.

41 C. Pothipor, *et al.*, An electrochemical biosensor for simultaneous detection of breast cancer clinically related microRNAs based on a gold nanoparticles/graphene quantum dots/graphene oxide film, *Analyst*, 2021, **146**(12), 4000–4009.

42 J. Wang, *et al.*, An ultrasensitive electrochemical biosensor for detection of microRNA-21 based on redox reaction of ascorbic acid/iodine and duplex-specific nuclease assisted target recycling, *Biosens. Bioelectron.*, 2019, **130**, 81–87.

43 K. Zhang, *et al.*, Label-free impedimetric sensing platform for microRNA-21 based on ZrO$_2$-reduced graphene oxide nanohybrids coupled with catalytic hairpin assembly amplification, *RSC Adv.*, 2018, **8**(29), 16146–16151.

44 M. N. Islam, *et al.*, Graphene-Oxide-Loaded Superparamagnetic Iron Oxide Nanoparticles for Ultrasensitive Electrocatalytic Detection of MicroRNA, *ChemElectroChem*, 2018, **5**(17), 2488–2495.

45 J. Liu, S. Bao and X. Wang, Applications of Graphene-Based Materials in Sensors: A Review, *Micromachines*, 2022, **13**(2), 184.

46 E. B. Bahadır and M. K. Sezgintürk, Applications of graphene in electrochemical sensing and biosensing, *TrAC, Trends Anal. Chem.*, 2016, **76**, 1–14.

47 H. A. Alhazmi, *et al.*, Graphene-based biosensors for disease theranostics: Development, applications, and recent advancements, *Nanotechnol. Rev.*, 2022, **11**(1), 96–116.

48 C. Zhang, *et al.*, Progress in miRNA Detection Using Graphene Material-Based Biosensors, *Small*, 2019, **15**(38), 1901867.

49 K. Deng, *et al.*, Sensitive electrochemical sensing platform for microRNAs detection based on shortened multi-walled carbon nanotubes with high-loaded thionin, *Biosens. Bioelectron.*, 2018, **117**, 168–174.

50 J. Wang and Y. Lin, Functionalized carbon nanotubes and nanofibers for biosensing applications, *TrAC, Trends Anal. Chem.*, 2008, **27**(7), 619–626.

51 M. Mohammadniaei, *et al.*, Electrochemical nucleic acid detection based on parallel structural dsDNA/recombinant azurin hybrid, *Biosens. Bioelectron.*, 2017, **98**, 292–298.

52 F. Hu, *et al.*, An electrochemical biosensor for sensitive detection of microRNAs based on target-recycled non-enzymatic amplification, *Sens. Actuators, B*, 2018, **271**, 15–23.

53 P. Gai, *et al.*, Integration of Biofuel Cell-Based Self-Powered Biosensing and Homogeneous Electrochemical Strategy for Ultrasensitive and Easy-To-Use Bioassays of MicroRNA, *ACS Appl. Mater. Interfaces*, 2018, **10**(11), 9325–9331.

54 L. Zhang, *et al.*, Recent progresses in electrochemical DNA biosensors for MicroRNA detection, *Phenomics*, 2022, **2**(1), 18–32.

55 L. Yang, *et al.*, Electrochemical sensor based on Prussian blue/multi-walled carbon nanotubes functionalized polypyrrole nanowire arrays for hydrogen peroxide and microRNA detection, *Microchim. Acta*, 2021, **188**(1), 1–12.

56 Z. Chen, *et al.*, Exonuclease-assisted target recycling for ultrasensitive electrochemical detection of microRNA at vertically aligned carbon nanotubes, *Nanoscale*, 2019, **11**(23), 11262–11269.

57 M. Sireesha, *et al.*, A review on carbon nanotubes in biosensor devices and their applications in medicine, *Nanocomposites*, 2018, **4**(2), 36–57.

58 J. N. Tiwari, *et al.*, Engineered carbon-nanomaterial-based electrochemical sensors for biomolecules, *ACS Nano*, 2016, **10**(1), 46–80.

59 S. E. Elugoke, *et al.*, Conductive Nanodiamond-Based Detection of Neurotransmitters: One Decade, Few Sensors, *ACS Omega*, 2021, **6**(29), 18548–18558.

60 X. Ma, *et al.*, Electrochemical detection of microRNAs based on AuNPs/CNNS nanocomposite with Duplex-specific nuclease assisted target recycling to improve the sensitivity, *Talanta*, 2020, **208**, 120441.

61 T. Hu, *et al.*, Enzyme catalytic amplification of miRNA-155 detection with graphene quantum dot-based electrochemical biosensor, *Biosens. Bioelectron.*, 2016, **77**, 451–456.

62 F. Farshchi, *et al.*, Flexible paper-based label-free electrochemical biosensor for the monitoring of miRNA-21 using core–shell Ag@Au/GQD nano-ink: a new platform for the accurate and rapid analysis by low cost lab-on-paper technology, *Anal. Methods*, 2021, **13**(10), 1286–1294.

63 H. Wang, *et al.*, Ultrasensitive electrochemical paper-based biosensor for microRNA via strand displacement reaction and metal-organic frameworks, *Sens. Actuators, B*, 2018, **257**, 561–569.

64 F. Jahanpeyma, *et al.*, An enzymatic paper-based biosensor for ultrasensitive detection of DNA, *Front. Biosci., Scholar Ed.*, 2019, **11**, 122–135.

65 S. Burai, *et al.*, Chiroptical Effect in Charge Transfer Processes in Chiral Carbon Dot-Doped Biopolymers: Application Toward Developing Chiral Electrodes, *J. Phys. Chem. C*, 2023, **24**, 11730–11735.

66 L. Zhou, *et al.*, Dual-amplified strategy for ultrasensitive electrochemical biosensor based on click chemistry-mediated enzyme-assisted target recycling and functiona-

lized fullerene nanoparticles in the detection of microRNA-141, *Biosens. Bioelectron.*, 2020, **150**, 111964.

67 J. Su, *et al.*, A Carbon-Based DNA Framework Nano–Bio Interface for Biosensing with High Sensitivity and a High Signal-to-Noise Ratio, *ACS Sens.*, 2020, **5**(12), 3979–3987.

68 W. Chen, *et al.*, Synthesis and applications of graphene quantum dots: a review, *Nanotechnol. Rev.*, 2018, **7**(2), 157–185.

69 C. Coutinho and Á. Somoza, MicroRNA sensors based on gold nanoparticles, *Anal. Bioanal. Chem.*, 2019, **411**(9), 1807–1824.

70 Y. Li, H. J. Schluesener and S. Xu, Gold nanoparticle-based biosensors, *Gold Bull.*, 2010, **43**(1), 29–41.

71 A. Yu, *et al.*, Nanostructured electrochemical sensor based on dense gold nanoparticle films, *Nano Lett.*, 2003, **3**(9), 1203–1207.

72 C.-C. Chang, *et al.*, Gold Nanoparticle-Based Colorimetric Strategies for Chemical and Biological Sensing Applications, *Nanomaterials*, 2019, **9**(6), 861.

73 Z. Lu, *et al.*, Amplified voltammetric detection of miRNA from serum samples of glioma patients via combination of conducting magnetic microbeads and ferrocene-capped gold nanoparticle/streptavidin conjugates, *Biosens. Bioelectron.*, 2016, **86**, 502–507.

74 J. Wang, *et al.*, Multiplexed electrochemical detection of MiRNAs from sera of glioma patients at different stages via the novel conjugates of conducting magnetic microbeads and Diblock oligonucleotide-modified gold nanoparticles, *Anal. Chem.*, 2017, **89**(20), 10834–10840.

75 S. Catuogno, *et al.*, Recent advance in biosensors for microRNAs detection in cancer, *Cancers*, 2011, **3**(2), 1877–1898.

76 S. Campuzano, M. Pedrero and J. M. Pingarrón, Electrochemical genosensors for the detection of cancer-related miRNAs, *Anal. Bioanal. Chem.*, 2014, **406**(1), 27–33.

77 G.-J. Zhang, *et al.*, Label-free direct detection of MiRNAs with silicon nanowire biosensors, *Biosens. Bioelectron.*, 2009, **24**(8), 2504–2508.

78 B. Bo, *et al.*, Triple signal amplification strategy for ultrasensitive determination of miRNA based on duplex specific nuclease and bridge DNA–gold nanoparticles, *Anal. Chem.*, 2018, **90**(3), 2395–2400.

79 H. Tang, *et al.*, Dual-signal amplification strategy for miRNA sensing with high sensitivity and selectivity by use of single Au nanowire electrodes, *Biosens. Bioelectron.*, 2019, **131**, 88–94.

80 B. Li, *et al.*, Two-stage cyclic enzymatic amplification method for ultrasensitive electrochemical assay of microRNA-21 in the blood serum of gastric cancer patients, *Biosens. Bioelectron.*, 2016, **79**, 307–312.

81 Y. Tao, *et al.*, Double-loop hairpin probe and doxorubicin-loaded gold nanoparticles for the ultrasensitive electrochemical sensing of microRNA, *Biosens. Bioelectron.*, 2017, **96**, 99–105.

82 S. Liu, *et al.*, Manufacturing of an electrochemical biosensing platform based on hybrid DNA hydrogel: Taking lung

cancer-specific miR-21 as an example, *Biosens. Bioelectron.*, 2018, **103**, 1–5.

83 S. Deng, *et al.*, In situ terminus-regulated DNA hydrogelation for ultrasensitive on-chip microRNA assay, *Biosens. Bioelectron.*, 2019, **137**, 263–270.

84 H. Zhang, *et al.*, Sensitive electrochemical biosensor for MicroRNAs based on duplex-specific nuclease-assisted target recycling followed with gold nanoparticles and enzymatic signal amplification, *Anal. Chim. Acta*, 2019, **1064**, 33–39.

85 M. Zouari, *et al.*, Competitive RNA-RNA hybridization-based integrated nanostructured-disposable electrode for highly sensitive determination of miRNAs in cancer cells, *Biosens. Bioelectron.*, 2017, **91**, 40–45.

86 H. V. Tran, *et al.*, Fabrication of a quinone containing layer on gold nanoparticles directed to a label-free and reagentless electrochemical miRNA sensor, *Anal. Methods*, 2017, **9**(18), 2696–2702.

87 Y. Wu, *et al.*, Enzyme spheres as novel tracing tags coupled with target-induced DNAzyme assembly for ultrasensitive electrochemical microRNA assay, *Anal. Chim. Acta*, 2016, **948**, 1–8.

88 M. Mohammadniaei, *et al.*, Relay-race RNA/Barcode gold nanoflower hybrid for wide and sensitive detection of MicroRNA in total patient serum, *Biosens. Bioelectron.*, 2019, 111468.

89 S. Su, Q. Sun, J. Ma, D. Zhu, F. Wang, J. Chao, C. Fan, Q. Li and L. Wang, Ultrasensitive analysis of microRNAs with gold nanoparticle-decorated molybdenum disulfide nanohybrid-based multilayer nanoprobes, *Chem. Commun.*, 2020, **56**(63), 9012–9015.

90 A. Sabahi, *et al.*, Electrochemical nano-genosensor for highly sensitive detection of miR-21 biomarker based on SWCNT-grafted dendritic Au nanostructure for early detection of prostate cancer, *Talanta*, 2020, **209**, 120595.

91 X.-X. Peng, *et al.*, Nanostructuring Synergetic Base-Stacking Effect: An Enhanced Versatile Sandwich Sensor Enables Ultrasensitive Detection of MicroRNAs in Blood, *ACS Sens.*, 2020, **5**(8), 2514–2522.

92 Y. T. Yaman, *et al.*, One-pot synthesized gold nanoparticle-peptide nanotube modified disposable sensor for impedimetric recognition of miRNA 410, *Sens. Actuators, B*, 2020, **320**, 128343.

93 C. Pothipor, *et al.*, A highly sensitive electrochemical microRNA-21 biosensor based on intercalating methylene blue signal amplification and a highly dispersed gold nanoparticles/graphene/polypyrrole composite, *Analyst*, 2021, **146**(8), 2679–2688.

94 Y. Song, *et al.*, Integrated individually electrochemical array for simultaneously detecting multiple Alzheimer's biomarkers, *Biosens. Bioelectron.*, 2020, **162**, 112253.

95 M. Daneshpour, K. Omidfar and H. Ghanbarian, A novel electrochemical nanobiosensor for the ultrasensitive and specific detection of femtomolar-level gastric cancer biomarker miRNA-106a, *Beilstein J. Nanotechnol.*, 2016, **7**, 2023–2036.

96 M. Daneshpour, B. Karimi and K. Omidfar, Simultaneous detection of gastric cancer-involved miR-106a and let-7a through a dual-signal-marked electrochemical nanobiosensor, *Biosens. Bioelectron.*, 2018, **109**, 197–205.

97 C. Coutinho and Á. Somoza, MicroRNA sensors based on gold nanoparticles, *Anal. Bioanal. Chem.*, 2019, **411**, 1807–1824.

98 P. Si, *et al.*, Gold nanomaterials for optical biosensing and bioimaging, *Nanoscale Adv.*, 2021, **3**(10), 2679–2698.

99 N. Momeni, *et al.*, A Review on Gold Nanoparticles-Based Biosensors in Clinical and Non-Clinical Applications, *Int. J. Eng. Mater. Manuf.*, 2022, **7**(1), 1–12.

100 M. El Aamri, *et al.*, Electrochemical biosensors for detection of microRNA as a cancer biomarker: Pros and cons, *Biosensors*, 2020, **10**(11), 186.

101 G. S. Geleta, A colorimetric aptasensor based on gold nanoparticles for detection of microbial toxins: an alternative approach to conventional methods, *Anal. Bioanal. Chem.*, 2022, **414**(24), 7103–7122.

102 M. Kus-Liśkiewicz, P. Fickers and I. Ben Tahar, Biocompatibility and cytotoxicity of gold nanoparticles: recent advances in methodologies and regulations, *Int. J. Mol. Sci.*, 2021, **22**(20), 10952.

103 A. Yaqub, *et al.*, Efficient Preparation of a Nonenzymatic Nanoassembly Based on Cobalt-Substituted Polyoxometalate and Polyethylene Imine-Capped Silver Nanoparticles for the Electrochemical Sensing of Carbofuran, *ACS Omega*, 2022, **7**(1), 149–159.

104 H. Li, *et al.*, Tuning laccase catalytic activity with phosphate functionalized carbon dots by visible light, *ACS Appl. Mater. Interfaces*, 2015, **7**(18), 10004–10012.

105 T. Gao, *et al.*, One-step detection for two serological biomarker species to improve the diagnostic accuracy of hepatocellular carcinoma, *Talanta*, 2018, **178**, 89–93.

106 R. Tian, Y. Li and J. Bai, Hierarchical assembled nanomaterial paper based analytical devices for simultaneously electrochemical detection of microRNAs, *Anal. Chim. Acta*, 2019, **1058**, 89–96.

107 L. Liu, *et al.*, Simple, sensitive and label-free electrochemical detection of microRNAs based on the in situ formation of silver nanoparticles aggregates for signal amplification, *Biosens. Bioelectron.*, 2017, **94**, 235–242.

108 A. Asadzadeh-Firouzabadi and H. R. Zare, Preparation and application of AgNPs/SWCNTs nanohybrid as an electroactive label for sensitive detection of miRNA related to lung cancer, *Sens. Actuators, B*, 2018, **260**, 824–831.

109 T. Kangkamano, *et al.*, Pyrrolidinyl PNA polypyrrole/silver nanofoam electrode as a novel label-free electrochemical miRNA-21 biosensor, *Biosens. Bioelectron.*, 2018, **102**, 217–225.

110 Q. Wen, *et al.*, Rapid and sensitive electrochemical detection of microRNAs by gold nanoparticle-catalyzed silver enhancement, *Analyst*, 2020, **145**(24), 7893–7897.

111 H. Park, *et al.*, Mesoporous gold–silver alloy films towards amplification-free ultra-sensitive microRNA detection, *J. Mater. Chem. B*, 2020, **8**(41), 9512–9523.

112 W. Cheng, *et al.*, Enzyme-free electrochemical biosensor based on double signal amplification strategy for the ultra-sensitive detection of exosomal microRNAs in biological samples, *Talanta*, 2020, **219**, 121242.

113 F. Hakimian and H. Ghourchian, Ultrasensitive electrochemical biosensor for detection of microRNA-155 as a breast cancer risk factor, *Anal. Chim. Acta*, 2020, **1136**, 1–8.

114 M. Wang, *et al.*, Duplex-specific nuclease assisted miRNA assay based on gold and silver nanoparticles co-decorated on electrode interface, *Anal. Chim. Acta*, 2020, **1107**, 23–29.

115 N. R. Panyala, E. M. Peña-Méndez and J. Havel, Silver or silver nanoparticles: a hazardous threat to the environment and human health?, *J. Appl. Biomed.*, 2008, **6**(3), 117–129.

116 T. A. Rocha-Santos, Sensors and biosensors based on magnetic nanoparticles, *TrAC, Trends Anal. Chem.*, 2014, **62**, 28–36.

117 V. Urbanova, *et al.*, Nanocrystalline iron oxides, composites, and related materials as a platform for electrochemical, magnetic, and chemical biosensors, *Chem. Mater.*, 2014, **26**(23), 6653–6673.

118 C. Zhou, *et al.*, Ultrasensitive lab-on-paper device via Cu/Co double-doped CeO_2 nanospheres as signal amplifiers for electrochemical/visual sensing of miRNA-155, *Sens. Actuators, B*, 2020, **321**, 128499.

119 L. Yu, *et al.*, Manipulations of DNA four-way junction architecture and DNA modified Fe_3O_4@Au nanomaterials for the detection of miRNA, *Sens. Actuators, B*, 2020, **313**, 128015.

120 Q. Jia, *et al.*, Polyoxometalate-derived MoS_2 nanosheets embedded around iron-hydroxide nanorods as the platform for sensitively determining miRNA-21, *Sens. Actuators, B*, 2020, **323**, 128647.

121 X. Ma, *et al.*, A label-free electrochemical platform based on the thionine functionalized magnetic Fe-NC electrocatalyst for the detection of microRNA-21, *Analyst*, 2021, **146**(14), 4557–4565.

122 Y.-Y. Bai, *et al.*, One-to-many single entity electrochemistry biosensing for ultrasensitive detection of microRNA, *Anal. Chem.*, 2019, **92**(1), 853–858.

123 M. K. Masud, *et al.*, Nanostructured mesoporous gold biosensor for microRNA detection at attomolar level, *Biosens. Bioelectron.*, 2020, **168**, 112429.

124 P. H. Cortés and S. R. Macías, *Metal-organic frameworks in biomedical and environmental field*, Springer, 2021.

125 X. Tang, *et al.*, Strand displacement-triggered G-quadruplex/rolling circle amplification strategy for the ultra-sensitive electrochemical sensing of exosomal microRNAs, *Microchim. Acta*, 2020, **187**(3), 1–10.

126 S. Ranjbari, *et al.*, A novel electrochemical biosensor based on signal amplification of Au HFGNs/PnBA-MXene nanocomposite for the detection of miRNA-122 as a biomarker of breast cancer, *Talanta*, 2023, **255**, 124247.

127 X. Peng, *et al.*, Magnetic Nanobeads and De Novo Growth of Electroactive Polymers for Ultrasensitive microRNA Detection at the Cellular Level, *Anal. Chem.*, 2020, **93**(2), 902–910.

128 P. Kannan, *et al.*, Nickel-phosphate pompon flowers nano-structured network enables the sensitive detection of microRNA, *Talanta*, 2020, **209**, 120511.

129 S. Yazdanparast, *et al.*, Experimental and theoretical study for miR-155 detection through resveratrol interaction with nucleic acids using magnetic core-shell nanoparticles, *Microchim. Acta*, 2020, **187**(8), 1–10.

130 S. Balaban Hanoglu, *et al.*, Recent Approaches in Magnetic Nanoparticle-Based Biosensors of miRNA Detection, *Magnetochemistry*, 2023, **9**(1), 23.

131 I. Gessner, *et al.*, Magnetic nanoparticle-based amplification of microRNA detection in body fluids for early disease diagnosis, *J. Mater. Chem. B*, 2021, **9**(1), 9–22.

132 E. W. Chuan Lim and R. Feng, Agglomeration of magnetic nanoparticles, *J. Chem. Phys.*, 2012, **136**(12), 124109.

133 A. E. Baumann, *et al.*, Metal-organic framework functionalization and design strategies for advanced electrochemical energy storage devices, *Commun. Chem.*, 2019, **2**(1), 1–14.

134 X. Fang, *et al.*, Nanocomposites of Zr(IV)-based metal–organic frameworks and reduced graphene oxide for electrochemically sensing ciprofloxacin in water, *ACS Appl. Nano Mater.*, 2019, **2**(4), 2367–2376.

135 X. Li, *et al.*, Electrochemical biosensor for ultrasensitive exosomal miRNA analysis by cascade primer exchange reaction and MOF@Pt@MOF nanozyme, *Biosens. Bioelectron.*, 2020, **168**, 112554.

136 T. Meng, *et al.*, An enzyme-free electrochemical biosensor based on target-catalytic hairpin assembly and Pd@UiO-66 for the ultrasensitive detection of microRNA-21, *Anal. Chim. Acta*, 2020, **1138**, 59–68.

137 M. Hu, *et al.*, CoNi bimetallic metal–organic framework as an efficient biosensing platform for miRNA 126 detection, *Appl. Surf. Sci.*, 2021, **542**, 148586.

138 W. Zhong, *et al.*, High electrochemical active Au-NP/2D zinc-metal organic frameworks heterostructure-based ECL sensor for the miRNA-522 detection in triple negative breast cancer, *Talanta*, 2023, **265**, 124875.

139 G. A. Udourioh, M. M. Solomon and E. I. Epelle, Metal organic frameworks as biosensing materials for COVID-19, *Cell. Mol. Bioeng.*, 2021, **14**(6), 535–553.

140 L. Du, *et al.*, Applications of functional metal-organic frameworks in biosensors, *Biotechnol. J.*, 2021, **16**(2), 1900424.

141 M. T. Ulhakim, *et al.*, Recent trend on two-dimensional metal-organic frameworks for electrochemical biosensor application, *J. Electrochem. Soc.*, 2020, **167**(13), 136509.

142 G. Deysher, *et al.*, Synthesis of Mo_4VAlC_4 MAX phase and two-dimensional Mo_4VC_4 MXene with five atomic layers of transition metals, *ACS Nano*, 2019, **14**(1), 204–217.

143 R. Zhang, J. Liu and Y. Li, MXene with great adsorption ability toward organic dye: an excellent material for constructing a ratiometric electrochemical sensing platform, *ACS Sens.*, 2019, **4**(8), 2058–2064.

144 F. Duan, *et al.*, Construction of the 0D/2D heterojunction of $Ti_3C_2T_x$ MXene nanosheets and iron phthalocyanine

quantum dots for the impedimetric aptasensing of microRNA-155, *Sens. Actuators, B*, 2020, **310**, 127844.

145 X. Yang, *et al.*, An electrochemical biosensor based on $AuNPs/Ti_3C_2$ MXene three-dimensional nanocomposite for microRNA-155 detection by exonuclease III-aided cascade target recycling, *J. Electroanal. Chem.*, 2020, **878**, 114669.

146 M. Mohammadniaei, *et al.*, Gold nanoparticle/MXene for multiple and sensitive detection of oncomiRs based on synergetic signal amplification, *Biosens. Bioelectron.*, 2020, **159**, 112208.

147 Q. Wu, *et al.*, Ultrasensitive electrochemical biosensor for microRNA-377 detection based on MXene-Au nano-composite and G-quadruplex nano-amplification strategy, *Electrochim. Acta*, 2022, **428**, 140945.

148 J. Yoon, *et al.*, Recent advances in MXene nanocomposite-based biosensors, *Biosensors*, 2020, **10**(11), 185.

149 A. Sinha, *et al.*, *MXene-based sensors and biosensors: next-generation detection platforms*, *Handbook of Nanomaterials in Analytical Chemistry*, Elsevier, 2020, pp. 361–372.

150 B. Xu, C. Zhi and P. Shi, Latest advances in MXene biosensors, *J. Phys.: Mater.*, 2020, **3**(3), 031001.

151 A. Sinha, *et al.*, MXene: An emerging material for sensing and biosensing, *TrAC, Trends Anal. Chem.*, 2018, **105**, 424–435.

152 M. Khalid, *et al.*, *Fundamental Aspects and Perspectives of MXenes*, Springer, 2022.

153 K. Chaturvedi, *et al.*, The Rise of MXene: A Wonder 2D Material, from Its Synthesis and Properties to Its Versatile Applications—A Comprehensive Review, *Top. Curr. Chem.*, 2023, **381**(2), 11.

154 L. Shen, P. Wang and Y. Ke, DNA Nanotechnology-Based Biosensors and Therapeutics, *Adv. Healthcare Mater.*, 2021, **10**(15), 2002205.

155 Y. Jiang, *et al.*, Highly sensitive electrochemical sensor for an miR-200c assay based on ligation-assisted DNA strand displacements, *ACS Sustainable Chem. Eng.*, 2021, **9**(28), 9257–9263.

156 J. Lu, *et al.*, An electrochemical biosensor based on tetra-hedral DNA nanostructures and G-quadruplex/hemin conformation for the ultrasensitive detection of microRNA-21 in serum, *Anal. Chem.*, 2019, **91**(11), 7353–7359.

157 L. Zhou, *et al.*, A label-free electrochemical biosensor for microRNAs detection based on DNA nanomaterial by coupling with Y-shaped DNA structure and non-linear hybridization chain reaction, *Biosens. Bioelectron.*, 2019, **126**, 657–663.

158 R. Tian, *et al.*, High performance electrochemical biosensor based on 3D nitrogen-doped reduced graphene oxide electrode and tetrahedral DNA nanostructure, *Talanta*, 2019, **194**, 273–281.

159 Y. L. Huang, *et al.*, Amperometric biosensor for microRNA based on the use of tetrahedral DNA nanostructure probes and guanine nanowire amplification, *Microchim. Acta*, 2017, **184**(8), 2597–2604.

160 D. Zeng, *et al.*, DNA tetrahedral nanostructure-based electrochemical miRNA biosensor for simultaneous detec-

tion of multiple miRNAs in pancreatic carcinoma, *ACS Appl. Mater. Interfaces*, 2017, **9**(28), 24118–24125.

161 X. Zhang, *et al.*, Novel 2D-DNA-nanoprobe-mediated enzyme-free-target-recycling amplification for the ultrasensitive electrochemical detection of microRNA, *Anal. Chem.*, 2018, **90**(15), 9538–9544.

162 P. Liu, *et al.*, Enzyme-Free Electrochemical Biosensor Based on Localized DNA Cascade Displacement Reaction and Versatile DNA Nanosheets for Ultrasensitive Detection of Exosomal MicroRNA, *ACS Appl. Mater. Interfaces*, 2020, **12**(40), 45648–45656.

163 L. Jiang, *et al.*, An electrochemical sensor based on enzyme-free recycling amplification for sensitive and specific detection of miRNAs from cancer cells, *Analyst*, 2020, **145**(9), 3353–3358.

164 S. Xu, *et al.*, One DNA circle capture probe with multiple target recognition domains for simultaneous electrochemical detection of miRNA-21 and miRNA-155, *Biosens. Bioelectron.*, 2020, **149**, 111848.

165 P. Miao and Y. Tang, Dumbbell hybridization chain reaction based electrochemical biosensor for ultrasensitive detection of exosomal miRNA, *Anal. Chem.*, 2020, **92**(17), 12026–12032.

166 J. Guo, C. Yuan, Q. Yan, Q. Duan, X. Li and G. Yi, An electrochemical biosensor for microRNA-196a detection based on cyclic enzymatic signal amplification and template-free DNA extension reaction with the adsorption of methylene blue, *Biosens. Bioelectron.*, 2018, **105**, 103–108.

167 J. Wang and N. Hui, Electrochemical functionalization of polypyrrole nanowires for the development of ultrasensitive biosensors for detecting microRNA, *Sens. Actuators, B*, 2019, **281**, 478–485.

168 X. Chen, *et al.*, Novel electrochemical nanoswitch biosensor based on self-assembled pH-sensitive continuous circular DNA, *Biosens. Bioelectron.*, 2019, **131**, 274–279.

169 Z. Shen, *et al.*, Highly sensitive and simultaneous detection of microRNAs in serum using stir-bar assisted magnetic DNA nanospheres-encoded probes, *Biosens. Bioelectron.*, 2020, **148**, 111831.

170 T. Bao, *et al.*, Metal-Mediated Polydopamine Nanoparticles–DNA Nanomachine Coupling Electrochemical Conversion of Metal–Organic Frameworks for Ultrasensitive MicroRNA Sensing, *Anal. Chem.*, 2021, **93**(40), 13475–13484.

171 Y. Chang, *et al.*, DNA Three-Way Junction with Multiple Recognition Regions Mediated an Unconfined DNA Walker for Electrochemical Ultrasensitive Detection of miRNA-182-5p, *Anal. Chem.*, 2021, **93**(38), 12981–12986.

172 P. Miao and Y. Tang, DNA walking and rolling nanomachine for electrochemical detection of miRNA, *Small*, 2020, **16**(47), 2004518.

173 H. Lu, *et al.*, Three-dimensional DNA nanomachine combined with toehold-mediated strand displacement reaction for sensitive electrochemical detection of miRNA, *Langmuir*, 2020, **36**(36), 10708–10714.

174 X.-L. Zhang, *et al.*, Dual 3D DNA Nanomachine-Mediated Catalytic Hairpin Assembly for Ultrasensitive Detection of MicroRNA, *Anal. Chem.*, 2021, **93**(41), 13952–13959.

175 B. Mohan, *et al.*, Nanomaterials for miRNA detection: the hybridization chain reaction strategy, *Sens. Diagn.*, 2023, **2**(1), 78–89.

176 P.-Y. Lin, *et al.*, Applications of triplex DNA nanostructures in sensor development, *Anal. Bioanal. Chem.*, 2022, **414**(18), 5217–5237.

177 D. Mathur, *et al.*, Uptake and stability of DNA nanostructures in cells: a cross-sectional overview of the current state of the art, *Nanoscale*, 2023, **15**(6), 2516–2528.

178 A. R. Chandrasekaran, *et al.*, DNA nanotechnology approaches for microRNA detection and diagnosis, *Nucleic Acids Res.*, 2019, **47**(20), 10489–10505.

179 D.-X. Wang, *et al.*, DNA nanostructure-based nucleic acid probes: construction and biological applications, *Chem. Sci.*, 2021, **12**(22), 7602–7622.

180 J. Dong, *et al.*, Sandwich-type microRNA biosensor based on graphene oxide incorporated 3D-flower-like MoS_2 and AuNPs coupling with HRP enzyme signal amplification, *Microchim. Acta*, 2022, **189**(1), 49.

181 S. K. Krishnan, *et al.*, A review on graphene-based nanocomposites for electrochemical and fluorescent biosensors, *RSC Adv.*, 2019, **9**(16), 8778–8881.

182 J. Yoon, *et al.*, Graphene/MoS_2 nanohybrid for biosensors, *Materials*, 2021, **14**(3), 518.

183 H. Gergeroglu, S. Yildirim and M. F. Ebeoglugil, Nano-carbons in biosensor applications: an overview of carbon nanotubes (CNTs) and fullerenes (C_{60}), *SN Appl. Sci.*, 2020, **2**, 1–22.

184 J. Huang, Y. Liu and T. You, Carbon nanofiber based electrochemical biosensors: A review, *Anal. Methods*, 2010, **2**(3), 202–211.

185 J. Y. Lim and S. S. Lee, Sensitive detection of microRNA using QCM biosensors: sandwich hybridization and signal amplification by TiO_2 nanoparticles, *Anal. Methods*, 2020, **12**(42), 5103–5109.

186 K. P. Castro, *et al.*, Low-dimensionality carbon-based biosensors: the new era of emerging technologies in bioanalytical chemistry, *Anal. Bioanal. Chem.*, 2023, 1–17.

187 Y.-P. Wei, Y.-W. Zhang and C.-J. Mao, A silver nanoparticle-assisted signal amplification electrochemiluminescence biosensor for highly sensitive detection of mucin 1, *J. Mater. Chem. B*, 2020, **8**(12), 2471–2475.

188 Y. Bai, T. Xu and X. Zhang, Graphene-based biosensors for detection of biomarkers, *Micromachines*, 2020, **11**(1), 60.

189 H. Beyrampour-Basmenj, *et al.*, Sensitive and convenient detection of miRNA-145 using a gold nanoparticle-HCR coupled system: computational and validations, *IEEE Trans. NanoBiosci.*, 2022, **22**(1), 155–162.

190 M. Banchelli, *et al.*, Molecular beacon decorated silver nanowires for the quantitative miRNA detection by a SERS approach, *Anal. Methods*, 2023, **15**(45), 6165–6176.

191 Y. Zhao, *et al.*, Metal–organic frameworks as photoluminescent biosensing platforms: mechanisms and applications, *Chem. Soc. Rev.*, 2021, **50**(7), 4484–4513.

192 L. Gutiérrez-Gálvez, *et al.*, Carbon nanodot-based electrogenerated chemiluminescence biosensor for miRNA-21 detection, *Microchim. Acta*, 2021, **188**, 1–12.

193 H. Malekzad, *et al.*, Noble metal nanoparticles in biosensors: recent studies and applications, *Nanotechnol. Rev.*, 2017, **6**(3), 301–329.

194 S. B. Yaqoob, *et al.*, Gold, silver, and palladium nanoparticles: a chemical tool for biomedical applications, *Front. Chem.*, 2020, **8**, 376.

195 Y. Wang, *et al.*, Ultrasensitive label-free miRNA-21 detection based on MXene-enhanced plasmonic lateral displacement measurement, *Nanophotonics*, 2023, **12**(21), 4055–4062.

196 L. Mo, *et al.*, Recent progress in the development of DNA-based biosensors integrated with hybridization chain reaction or catalytic hairpin assembly, *Front. Chem.*, 2023, **11**, 1134863.